Carbon Consumption, the Carbon-Based Ecosystem, and Output

Cristian Figueroa, Rodrigo Harrison, Roger Lagunoff, and Mario J. Miranda*

Draft of August 20, 2019

Abstract

This paper studies the effects of changes in the carbon-based ecosystem on a country's output. We propose and estimate a dynamic production model in which a country's ecosystem, as measured by its reservoir of carbon in land biomass and soils, enters explicitly as a productive input. Land use is the key endogenous decision in the model. We characterize a country's optimal land use policy given its direct effects on the ecosystem, and the indirect feedback effects from land sink absorption of atmospheric GHG concentrations. We estimate the model's land sink absorption rates and output elasticities with respect to land use, fossil fuel emissions, and land carbon stock for 162 countries. Globally, a 1% decline in a country's land carbon leads to an estimated 0.3% decline in its GDP per year, even after it optimally adjusts its land use policy. We then simulate the model to 2100 under four standard Representative Concentration Pathway scenarios. In the simulations, developed countries experience higher GDP growth by 2100 under low concentration scenarios. For these countries, GDP initially grows faster in high concentration scenarios. By 2050 it declines in high concentration scenarios but continues to grow in low ones. Developing countries, by contrast, experience higher GDP growth under high concentration scenarios throughout the century. Global growth in GDP is maximal under low to moderate GHG concentration scenarios.

Key words: Carbon-based ecosystem, land stocks, GHG emissions, optimal land use policy, policy-adjusted elasticity, Representative Concentration Pathways.

---

*The authors are, respectively, doctoral student, Boston College, Professor, Facultad de Ingeniería y Ciencias Universidad Adolfo Ibañez, Professor, Georgetown University, and Professor, The Ohio State University. We thank Hans Schlechter and Rodrigo Yáñez for valuable research assistance.

1 Introduction

Studies of the effects of greenhouse gas emissions on economic outcomes are numerous. The effects are typically quantified in a class of integrated assessment models (IAMs) that incorporate an environmental damage function into a general equilibrium growth model.[1] Damage to output is postulated to be an increasing function of global surface temperature. In turn, surface temperature increases with greenhouse gas (GHG) concentrations from energy use. The estimated parameters of this function are then used to calibrate the long run effects of climate change on output.[2]

The damage function is a shorthand representation of an economy's sensitivity to changes in the ecosystem brought about by climate change. Viewed as a "capital stock", the ecosystem maintains the resiliency of a country's economy by preserving soil nutrients, preventing erosion, flooding, and habitat loss, acting as filtration system for human and animal waste, and serving as a natural climate stabilizer (IPCC, 2014; Mcalpine and Wotton, 2009).

This paper proposes and estimates a dynamic growth model where each country's policymakers account for the carbon based ecosystem. The ecosystem, comprising the reservoir of un-extracted carbon contained in land biomass and soils, enters the model explicitly as a productive input along with two others: fossil fuel consumption and land use. The three inputs directly increase output. Our study focusses on the indirect effects of fossil fuels and land use on the ecosystem. Namely, the resulting increases in global atmospheric GHGs can lead to land carbon depletion, consequently degrading a key productive input for GDP growth.

This feedback channel works through sink absorption or *sequestration*. Land sink absorption, the ability of land biomass to absorb carbon from the atmosphere, arises from a subtle combination of plant photosynthesis and respiration and ground absorption of carbon. The process is not negligible. The world's stock of carbon biomass, both above and below ground, in 2010 was approximately 1260 Gt CO2e (FAO (2015) and Zomer et al. (2016)). The land sink flow for 2011 constituted around 0.8% of the 2010 stock, excluding anthropogenic responses (Le Quere et al., 2018). All else equal, greater absorption capacity can increase the terrestrial stock and reduce atmospheric GHGs. Thus, a land sink with greater absorption capacity can, to some degree, reduce climate change and/or mitigate its effects.

[1] Recent economic studies and integrated assessment models of this type include Krusell and Smith (2009); Dell, Jones, and Olken (2012); Golosov et al. (2014); Acemoglu et al. (2012); Cai, Judd, and Lontzek (2012); IPCC (2014); Burke, Hsiang, and Miguel (2015); Cai et al. (2015); Hsiang et al. (2017); Deryugina and Hsiang (2017); Nordhaus (2018), and many others.

[2] See Nordhaus (2013) for a more complete description.

The absorption capacity of the sinks, however, depends on the existing concentration of atmospheric GHGs. A number of studies indicate that increases in atmospheric GHGs may initially increase, but would eventually decrease, the reabsorption rates of carbon into plant and soils (Hikosaka et al., 2006; Thomson et al., 2008; Fernandez-Martinez et al., 2017; Raupach et al., 2014; Xu, 2015; Feng et al., 2015; Zheng et al., 2018). At some point, high enough concentrations hinder the capacity of the terrestrial ecosystem to absorb GHGs from the atmosphere. In the extreme, sinks can turn negative: respiration and decomposition outweigh absorption and photosynthesis.[3]

The paper posits and estimates a "sequestration" function from atmospheric greenhouse gases to the country's land sink. Using the data from 2018 Global Carbon Project, the estimated coefficients of the function are statistically significant and are consistent with a single peaked relationship between the GHG concentrations and land sink.

Land use is the key endogenous policy decision in the model. It encompasses a wide array of activities, including agriculture, forestry, freshwater fisheries, and urban development. While integrated assessment climate models include a highly developed energy sector, there are "far fewer land-use [climate] scenarios published in the literature than emission or energy-use scenarios" (van Vuuren et al., 2011). Land use becomes central in our study precisely because optimal land use policies must trade off immediate positive effects of land use and emissions against the longer run negative consequences of diminished terrestrial carbon stocks.

An *optimal land use policy* for a country is a pair of state-contingent choices on land emissions and atmospheric removals (from replanting, reseeding, etc) that maximize discounted dynamic payoffs of its representative consumer. Externalities arise because countries do not internalize the effects of their decisions on other countries' local ecosystems. Nor can they fully internalize the indirect feedback of other countries' ecosystems on their own.

Optimal land policies are shown to exist and are characterized in closed form. Optimal land emissions increase in land carbon stock and in land sink, while optimal removals decrease in both. Net emissions (emissions minus removals) decrease in the output elasticity of the ecosystem and decrease in the discount factor. In other words, preserving the ecosystem is desireable both because of its direct value as an input, and because of its indirect value in smoothing inter-temporal consumption.

Using data on carbon stocks from the Food and Agriculture Organization of the

[3]In one example, recent droughts and beetle infestation related to droughts, have resulted in the forests of six states in the U.S., Arizona, Colorado, Montana, Nevada, Utah, and Wyoming, becoming sources, rather than sinks, for emissions (Mooney and Murphy, 2019).

United Nations (FAO, 2019) we structurally estimate the model's output elasticities for 162 countries covering the time period 1990-2015. We obtain pooled estimates of elasticities, with country-fixed dummies, for each of four clusters of countries. Each country cluster is grouped according to the United Nations Human Development Index (HDI). A country is categorized as either High, Medium High, Medium Low, or Low development. Estimates are also obtained when countries are grouped by emissions, forestry stock, geography, GDP, and OECD inclusion.

The key parameter of interest is the *policy-adjusted output elasticity of land carbon*. It quantifies the effect of a percentage increase in the country's land carbon stock, as measured by its CO2e content, on GDP after adjusting for optimal land use. Since the stock affects GDP both directly as an input and indirectly via the country's land use policy, the policy-adjusted elasticity determines the *net* effects from both anthropogenic and non-anthropogenic changes in the ecosystem.

Endogenous land policy turns out to be critical for identifying the policy-adjusted elasticity. Country data does not distinguish exogenous land sinks from endogenous behavior. Nor does it distinguish between emissions and removals. Without endogenous policy in the model, it would be difficult to disentangle exogenous and endogenous sources and sinks.

The estimates of policy-adjusted elasticities are positive and statistically significant over the entire sample. They are also positive and statistically significant in the High and Medium High Development country clusters. The measured elasticity in these clusters are positive and sizable. Applied to the U.S., for instance, the observed increase in U.S. land carbon stock from 2010 to 2015 accounted for annual GDP growth of 0.28%. In China, the figure was around 1.14%.

Estimates of the policy adjusted elasticity are not statistically significant for low and medium low development countries although the model's overall fit is high. In those countries the relation between the country's ecosystem and its GDP is more tenuous over the time period in the data.

To assess long run effects, we calibrate the model to the elasticity and land sink estimates and run simulations of output by country cluster from 2020 to the end of the century. The simulations are run under alternative scenarios corresponding to the standard four Representative Concentration Pathways (RCPs) used for the Intergovernmental Panel on Climate Change Fifth Assessment (IPCC, 2014). Each RCP is based on distinct scenarios for growth in fossil fuel and energy consumption, population, land emissions, mitigation investments, and climate policy (van Vuuren et al., 2011). The RCPs are labeled according to their projected levels radiative forcing achieved at the end of the century, relative to pre-industrial levels. Low GHG concentration scenarios incorporate assumptions on improvements in mit-

igation technology and/or successful policy coordination. High GHG concentration scenarios are based on business-as-usual assumptions.

Taking 2015 data as the initial state we incorporate model-generated land use policies for each RCP scenario. Then using parameter estimates for production and sequestration, we simulate dynamic paths of land stocks, land sink absorption rates, and GDP for each HDI country cluster from 2020 to the end of the century.

The resulting forecasts show continued GDP growth for all HDI clusters until mid-century, after which time they diverge, depending on the emissions scenario and on the country's level of development. In highly developed countries, GDP growth is around 1.1% under high concentration scenarios until 2050, at which point GDP peaks and then falls dramatically due to declines in land carbon (eco-capital) stock. The higher the RCP, the higher/earlier the peak and the faster the decline.

The high concentration scenarios are therefore detrimental for developed countries in the second half of the century. By contrast, the low RCP scenario, which incorporates technological improvements in mitigation and earlier peaks in fossil fuel use, are beneficial.[4] Growth in highly developed countries' GDP in low emissions scenarios continue after mid-century, averaging just under 1% annually to 2100. Countries in the medium development group experience similar growth trends.

In contrast to the high development clusters, the low development clusters experience continued growth of around 2% in the high GHG concentration scenarios, and slight declines in low ones. The trend at the end of the century suggests that growth for the low development countries will be highest in the moderate concentration scenarios over the very long run.

Simulations under other clustering strategies are consistent with those generated using the Human Development Index. Overall, they indicate that the lowest emissions scenarios produces higher long run GDP for the developed countries, while moderate to high concentration scenarios produce higher long run GDP for developing countries. When aggregating across development clusters, the simulations show global GDP by 2100 at its highest in the low to moderate concentration scenarios. One takeaway is that in order to attain globally maximal GDP, substantial transfers from developed to developing countries may be necessary.

We emphasize that these conclusions only concern GDP. Althor, Watson, and Fuller (2016) develop alternative indices relating to a country's vulnerability to climate change. Indices of sensitivity to land use are analyzed by Canadell et al. (2007); Thomson et al. (2008); Ito et al. (2008); Power (2010); Zomer et al. (2016); FAO (2015); Narayan et al. (2017). The general consensus in this literature is that

[4]Estimates by Mohr et al. (2015) suggest the lower scenarios to be more consistent with geological estimates of fossil fuel availability.

low rather than high development countries are more vulnerable to climate change and to ecological damage more generally.

Our findings are not inconsistent with these published results. We show that developing countries experience greater deterioration of land carbon under high concentrations scenarios even as growth in GDP continues. In other words, high concentrations scenarios may make developing countries both more vulnerable *and* materially better off over the next half century.

Finally, we conduct a simple counterfactual experiment by holding land sink fixed at its average rate across the sample period. By doing so, we assess how much of the variation in GDP in our simulations are due to the deterioration land sink absorption rates. The results are striking. Unlike the active (inverted-U) sink model, there are no reversals or sharp declines in the higher concentration scenarios. In the constant sink model, high concentration scenarios display higher GDP growth than lower ones at every point in time. Comparing the best growth scenarios for each of the two land sink models, the simulations show that by the end of the century global output under active sink model is less than a third of what it would be if sink absorption changes were not a factor. Thus, long run prospects for GDP growth appear highly sensitive to the combination of environmental and human responses to GHG concentrations.

The paper is organized as follows. Section 2 develops the model, starting with a rudimentary model of the carbon cycle together with a dynamic model of optimal carbon policy. This includes a description of country-specific production processes that incorporate the carbon-based inputs described above. The structural equations and identification strategy are described in Section 3. Section 4 describes the data and the estimation results. Section 5 describes the simulation procedure, the use of RCP projections, and results. A summary discussion in Section 6 concludes the paper. The Appendix at the end contains proofs, further documentation, and a full description of the algorithms used to estimate and simulate the model.

2 A Dynamic Model of Carbon Consumption

This section presents a discrete time, infinite horizon model of carbon consumption among n countries. Each country consumes carbon in the form of fossil fuels and land use. Consumption interacts with natural feedback channels to determine the evolution of the terrestrial carbon ecosystem over time.

At each decision date $t = 0, 1, 2, \ldots$, a country faces a dynamic trade-off between the positive effects of carbon consumption and the negative effects on its terrestrial ecosystem from that consumption. A country chooses a dynamically optimal land

policy given this trade off and given the feedback effects from global accumulation of GHGs in the atmosphere.

On some dimensions, the model is simpler than most IAMs. It does not contain a highly detailed and disaggregated energy sector. Energy pricing and market outcomes are exogenous. Endogenous choices are limited to land policies. These simplifications increase the transparency of the dynamic trade offs for optimal policy making. In particular, policy choices in the model are endogenously determined by rational, forward looking authorities who are cognizant of the dynamic changes to their environment. The trade offs they face are characterized by interpretable Euler equations.

All decisions take place in a rudimentary model of the carbon cycle. The model laid out before proceeding with the economic model.

2.1 Global Carbon Accounting

In standard methods of carbon accounting, the global stock of carbon is constant. The carbon cycle shifts various portions of the stock to various reservoirs. This, in turn, defines a mass balance equation at each date t, represented as a sum of fluxes, i.e., net changes in the various components which cancel out in the aggregate:

$$0 = (\omega_t^{lan} - \omega_{t-1}^{lan}) + (\omega_t^{atm} - \omega_{t-1}^{atm}) + (\omega_t^{mar} - \omega_{t-1}^{mar}) + (\omega_t^{fos} - \omega_{t-1}^{fos}) \tag{1}$$

where ω_t^{lan} denotes the land carbon stock at t. It comprises the terrestrial stock of carbon found in plants, animals, leaf litter, and organic matter in soils. The stock ω_t^{atm} is the atmospheric carbon stock at t, while ω_t^{mar} refers carbon content in oceans. The variable ω_t^{fos} is the below-ground stock of from fossil fuels.[5] All carbon stocks are measured in a common unit.[6]

Many of the regulating forces that determine (1) are non-anthropogenic, including plant photosynthesis and respiration and carbon diffusion between oceans and atmosphere. However, these flows are also influenced by human activities.

First, the change in the fossil fuel reservoir is determined by human consumption,

$$\omega_{t-1}^{fos} - \omega_t^{fos} = c_t^{fos} \tag{2}$$

[5]Due to seasonal variations or measurement error the measured carbon budget in any given year may not be in balance (Le Quere et al., 2018). In a longer time scale, the total stock would include geological carbon, that is, non-fossil fuel sources of carbon contained in the earth's crust. It accumulates too slowly to be relevant for the human time scale.

[6]Gigatonnes of CO2 equivalent (Gt CO2e). See Appendix for definitions.

where c_t^{fos} represents global carbon emissions from fossil fuels consumption.[7] The stock is not fully known and estimates have steadily risen since 1980 (British Petroleum, 2019). Second, the change in land biomass is determined by both exogenous and anthropogenic sources. Formally:

$$\omega_t^{lan} = \omega_{t-1}^{lan} - (c_t^{lan} - r_t^{lan}) + s_t^{lan}. \tag{3}$$

The anthropogenic sources c_t^{lan} and r_t^{lan} constitute consumption/emissions from and removals toward land carbon stocks at date t. Land consumption is measured by atmospheric emissions from activities such as deforestation, agricultural harvests, animal husbandry, and natural resource extraction. Removals (from the atmosphere) includes reforestation, replanting, and preservation. Logically, the emissions and removals activities must be distinguished since removals are akin to an investment in future capacity and so it does not directly enter into current output of any country. The difference $c_t^{lan} - r_t^{lan}$ accounts for land use change and forestry (LUCF).[8]

The term s_t^{lan} is the global *land sink* representing non-anthropogenic removals from the atmosphere. It comprises the total net carbon absorption by unmanaged biomass due to photosynthesis and other factors. By definition it excludes LUCF.

Ito et al. (2008) describes land sink as a "wide range of environmental changes which include climate change (water and temperature), disease outbreaks, added nutrients (CO2 and nitrates), pollution damage (O3), and re-growth of vegetation in natural (unmanaged) land that is not included under the UNFCCC reporting guidelines for LULUCF." The definition is broad. It accounts for most of the feedback effects of climate change that are not directly associated with contemporaneous changes to the ecosystem by humans.

Both land use and fossil fuel consumption alter the mass balance equation by altering the flows into/out of land, fossil fuel, and atmospheric stocks directly. The land sink links atmospheric carbon to terrestrial carbon stocks via a subtle feedback mechanism.

Recent results from Hikosaka et al. (2006) Raupach et al. (2014), Xu (2015), and Zheng et al. (2018) indicate an inverted-U relationship between atmospheric carbon stock ω_{t-1}^{atm} and the *land sink absorption rate*, $\rho_t \equiv s_t^{lan}/\omega_{t-1}^{lan}$, the land sink per unit of land stock entering the period. The absorption rate ρ_t can be either positive or negative, taking values in $[-1, \infty)$. Negative values correspond to respiration and decomposition rates that exceed in total the rate of photosynthesis. At low atmospheric concentrations, increases in CO2e in the atmosphere increases the activation energy

[7] The stock ω_t^{fos} cannot be replenished on the human time scale.

[8] Following upgraded measurement, the United Nation's new designation is "Land use, land use change, and forestry" (LULUCF), though the original terminology still dominates the literature.

in plant photosynthesis. Consequently, carbon uptake (photosynthesis net of plant respiration) rises. After some point, however, increased GHG concentrations become toxic and higher temperatures deplete nutrient and moisture retention which further reduces uptake. Related mechanisms are studied by Fernandez-Martinez et al. (2017), Thomson et al. (2008), and Feng et al. (2015). To account for these effects, we posit

$$\rho_t \equiv \frac{s_t^{lan}}{\omega_{t-1}^{lan}} = F(\omega_{t-1}^{atm}; \pi) \tag{4}$$

where F is a continuous, single peaked function of ω_{t-1}^{atm} and π is a vector of parameters.

We will refer to F as the *sequestration function*. For the simulations, we later estimate the parameter vector π for a flexible functional form meeting the criteria above. To isolate the effects on land carbon, the sequestration function (4) is the only feedback mechanism in the model. Other feedback effects on, say, marine ecosystems, are not incorporated.

Combining equations (2), (3), and (4) with the mass balance equation (1) one obtains a rudimentary version of the land-atmospheric carbon cycle. The channels for this cycle are illustrated in Figure 1.

2.2 Output and Optimal Land Use Policies

Land emissions and removals are choices made by countries and depend on the country's stock of terrestrial carbon found in biomass and soils. Adding an "i" subscript to each of the variables, we obtain country i's land carbon stock ω_{it}^{lan} at the end of period t, its land and fossil fuel emissions c_{it}^{lan} and c_{it}^{fos}, its removals r_{it}^{lan}, and its land sink s_{it}^{lan}. These aggregate up to global stocks and flows as expected: $\omega_t^{lan} = \sum_i \omega_{it}^{lan}$, $c_t^{fos} = \sum_i c_{it}^{fos}$, $c_t^{lan} = \sum_i c_{it}^{lan}$, $r_t^{lan} = \sum_i r_{it}^{lan}$, and $s_t^{lan} = \sum_i s_{it}^{lan}$.

The country-specific version of the land stock dynamic in Equation (3) is

$$\omega_{i,t}^{lan} = \omega_{i,t-1}^{lan} - (c_{it}^{lan} - r_{i,t}^{lan}) + s_{it}^{lan}. \tag{5}$$

Like their global counterparts, c_{it}^{lan} incorporates activities such as harvesting, soil drainage, and deforestation within country i, while r_{it}^{lan} includes replanting, reseeding, and reforestation. The land sink s_{it}^{lan} of country i represents non-anthropogenic removals from the atmosphere that feed directly to the country's land stock.

At the country level, human activities enter into a country's output each period. The output y_{it} of country i is generated by the production function

$$y_{it} = A_i \varepsilon_{i,t} (c_{it}^{lan})^{\alpha_i} (\omega_{it}^{lan})^{\beta_i} (c_{it}^{fos})^{\gamma_i} L_{it}^{\phi_i}. \tag{6}$$

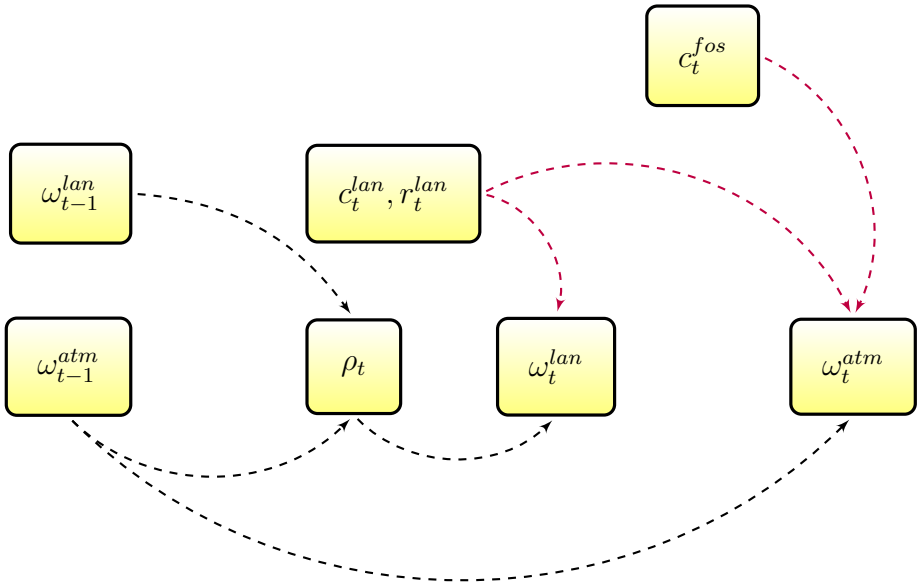

Figure 1: A Rudimentary Carbon Cycle (without ocean sinks).

In this expression, A_i is a TFP scale parameter for country i and $\varepsilon_{i,t}$ is a log normally distributed iid shock with mean 1. Labor L_{it} is directly included as a standard input. Traditional (constructed) capital stock does not appear in (6) but enters indirectly as a service flow reflected in fossil fuel consumption c_{it}^{fos} that requires capital to generate emissions.[9] The land carbon stock ω_{it}^{lan} enters the production technology directly as an input and so there are tangible, contemporaneous losses when the stock is diminished.[10]

The coefficients $\alpha_i, \beta_i, \gamma_i$, and ϕ_i would generally be expected to differ across

[9]More precisely, if it were the case that c_{it}^{fos} is endogenous then the absence of man-made capital would be a serious omission since capital stock imposes structure on an agent's choice of service flow. However, in our partial equilibrium setup, c_{it}^{fos} is exogenous. This means there is no constrained decision problem for agents, and for estimation purposes variations physical capital K_t are reflected in variations in c_{it}^{fos}.

[10]In pure extraction models, e.g. Levhari and Mirman (1980), Cave (1987), Fisher and Mirman (1992), conservation is valued for instrumental reasons: preserving the stock allows the decision maker to smooth consumption. The non-instrumental trade offs modeled are somewhat similar to models of Dutta and Radner (2004, 2006, 2009) who study dynamic strategic models of energy usage with emissions externalities, and Harrison and Lagunoff (2017, 2019) who also incorporate carbon stock as productive input.

countries. To maintain large enough sample sizes in the estimation stage, countries with similar development and/or geographic characteristics will be assumed to have the same elasticity profile. For estimation, various methods are used for grouping countries according to level of development, geography, resource endowment, or trade connections. These are described in Section 4.

Combining the output equation with the law of motion for carbon stock in Equation (5), we obtain

$$y_{it} = A_i \varepsilon_{it} (c_{it}^{lan})^{\alpha_i} \left(\omega_{i,t-1}^{lan} - c_{it}^{lan} + r_{it}^{lan} + s_{it}^{lan}\right)^{\beta_i} (c_{it}^{fos})^{\gamma_i} L_{it}^{\phi_i}. \tag{7}$$

Land consumption c_{it}^{lan} appears as both a direct and indirect input, the latter entering negatively through the land stock.

A policymaker from country i maximizes the discounted long run payoff

$$\sum_{t=0}^{\infty} \delta^t \left[\log(y_{it}) + \theta_i \log(\omega_{i,t-1}^{lan} - r_{it}^{lan})\right]. \tag{8}$$

Equation (8) is a reduced form payoff defined directly over output. The first term is i's flow payoff from y_{it}. The second term is its payoff from services derived from land stock net of efforts (removals) to expand it. This term is the payoff from home production or, alternatively, the payoff from eco-services including tourism, outdoor leisure, and general enjoyment of green space. Home production is relevant in developing countries where the land ecosystem is a non-monetized input that maintains soil stability, water filtration, and so on. The practical effect of this term is that is creates a trade off in the choice of r_{it}^{lan}.

At each date, a country chooses land activities c_{it}^{lan} and r_{it}^{lan} optimally, taking as given fossil fuel consumption c_{it}^{fos}, land sink s_{it}, and labor L_{it}.

A *land carbon policy* for country i is a pair of contingent maps $\mathbf{c_i^{lan}}$ and $\mathbf{r_i^{lan}}$ from the initial stock $\omega_{i,t-1}^{lan}$ and land sink s_{it}^{lan} to land emissions and removals, respectively. Given its chosen land policy, the country's Bellman equation is

$$\begin{aligned} V_i(\mathbf{c_i^{lan}}, \mathbf{r_i^{lan}}; \omega_{i,t-1}^{lan}, s_{it}^{lan}) = \max_{c_{it}^{lan}, r_{it}^{lan}} \big\{ & \alpha_i \log(c_{it}^{lan}) \\ & + \beta_i \log\left(\omega_{i,t-1}^{lan} + r_{i,t}^{lan} + s_{it}^{lan} - c_{it}^{lan}\right) + \theta_t \log(\omega_{i,t-1}^{lan} - r_{it}^{lan}) \\ & + \gamma_i \log(c_{it}^{fos}) + \phi_t \log(L_{it}) + \delta \; E\left[V_i(\mathbf{c_i^{lan}}, \mathbf{r_i^{lan}}; \omega_{i,t}^{lan}, s_{i,t+1}^{lan})\right] \big\} \end{aligned} \tag{9}$$

Equation (9) omits constant term $\log(A_i)$ and current log productivity shock $\log(\epsilon_{it})$. While we attribute a structural interpretation for the shock, under the log normal

assumption the expected future stream of payoffs over the shocks is zero and so it will not figure in the policymaker's decision problem.

An *optimal land policy* is a land policy that maximizes the representative citizen's long run payoff at each t for every stock $\omega_{i,t-1}^{lan}$ and sink s_{it}^{lan}, given the law of motion in (5) for land carbon. The optimization problem (9) relies on a few key assumptions:

- The policymaker maximizes output rather than consumption or some broader measurement of welfare. The simplifying assumption allows one to compare GDP across countries and across time under GDP-maximizing land use decisions. To make the model tractable, other measures of socio-economic costs are omitted. Consequently, the estimates reported here can be viewed as a lower bound on the true damages from degraded land stocks.

- Land use is determined by a policymaker. This is essential to the identification strategy. By assuming that government can optimally respond to changes in the terrestrial ecosystem, we analyze a "best-case" mitigation policy. To the extent that actual land use is not optimal, the estimates can be viewed as a lower bound on true damages. The assumption is also a reasonable approximation of the power of national governments in determining land use. The bulk of carbon biomass is on nationally owned land. In China, for instance, more than half of its territory and nearly all its forest land is publicly owned by the state. In the U.S. 28% of its territory and most of its forested areas are nationally held, and this excludes property held by various state governments (Rights and Resources Initiative, 2015; Vincent, Hanson, and Argueta, 2017). Even when property is privately held, federal laws governing pollutants, forestry, water and waste management, eminent domain, zoning restrictions, safety, building codes, and an array of subsidies and taxes implicate government in virtually all forms of land use.

- Global atmospheric CO2e concentrations are exogenous to each country's optimization problem. This is partly for tractability. Globally, LUCF is a small fraction of total emissions and a tiny fraction of the total atmospheric GHGs. The effects of any particular country's land policy at a point in time is even smaller. Consequently, the optimization problem (9) excludes the effects of its choice of c_{it}^{lan} on future atmospheric concentrations.[11]

[11]The assumption does not imply that a country regards its own land sink as exogenous. By Equation (4), land sinks are proportional to carbon stock, and the effects of an incremental change in its own carbon stock are fully internalized by the country.

- In this partial equilibrium framework, fossil fuel use and labor are exogenous to a country's land carbon policy. Fossil fuel use and labor are then determined in the global market rather than the result of a country's decision problem. One could point to general carbon tax policies that simultaneously affect both fossil fuel and land use emissions. Carbon taxes, however, are difficult to apply to land uses at the source. Unlike fossil fuel emissions, measurements of land carbon emissions typically do not or cannot disentangle endogenous from exogenous factors.[12] Moreover, targeted land use policies (e.g., licensing, zoning, leasing fees) are often available. Consequently, model treats fossil fuel policies as a separate policy problem outside the scope of the model.

The following proposition establishes that the country's optimization problem admits a simple closed form solution:

Proposition 1 *An optimal land carbon policy for country i is given by*

$$\begin{aligned} \mathbf{c}_{it}^{lan}(\omega_{i,t-1}^{lan}, s_{it}^{lan}) &= \frac{\alpha_i(1-\delta)(2\omega_{i,t-1}^{lan} + s_{it}^{lan})}{\alpha_i + \beta_i + \theta_i} \\ \mathbf{r}_{it}^{lan}(\omega_{i,t-1}^{lan}, s_{it}^{lan}) &= \omega_{i,t-1}^{lan} - \frac{\theta_i(1-\delta)(2\omega_{i,t-1}^{lan} + s_{it}^{lan})}{\alpha_i + \beta_i + \theta_i}. \end{aligned} \tag{10}$$

The optimal land policy exists whenever $\alpha_i > 0$ and $\alpha_i + \beta_i + \theta_i > 0$. If $\beta_i > 0$ then $\theta_i > 0$.

The derivation of (10) is in Appendix 7.1. A country's optimal land emissions and removals are multilinear functions of lagged land stock $\omega_{i,t-1}^{lan}$ and current land sink s_{it}. Emissions (removals) are decreasing (increasing) in the discount factor since the upside to removals comes in the future.

Recall that α_i, the production coefficient on land emissions, represents that output responsiveness to increases in land emissions. In fact, both emissions and removals are increasing in α_i, The increase in removals owes to the fact that removals represent a re-investment in land carbon that enables increased land consumption in the future.

Parameter β_i, the coefficient on land stock, represents output responsiveness to the ecosystem. An increase in β_i decreases emissions but increases removals.

[12]Non-carbon GHG's such as nitrous oxide, an important source of land emissions, is typically excluded from carbon tax policies.

Existence of equilibrium requires some parametric restrictions. If $\alpha_i \leq 0$ then the country should generate no land use emissions. If $\beta_i > 0$ and $\theta_i \leq 0$ then the country should accumulate an unbounded volume of biomass. If $\alpha_i + \beta_i + \theta_i < 0$, then the country should immediate deplete its land stock. Payoffs are ill-defined in these cases.

Note that the cases $\beta_i < 0$, and even $\alpha_i + \beta_i < 0$ are consistent with existence of an optimal land policy. Changes in land stock can be negatively related to *measured* GDP growth due the presence of home/non-monetized production. With home production, a reduction in land biomass can lead to greater substitution toward monetized output and away from home production. This "substitution effect" is likely more prevalent in developing countries and could produce a sum $\alpha_i + \beta_i$ that's negative. In that case, θ_i must be large relative to $|\beta_i|$ so that the sum $\alpha_i + \beta_i + \theta_i$ remains positive.

Later on, the model is specialized to the case where land sink absorption rates $s_{it}^{lan}/\omega_{t-1}^{lan}$ are identical across countries. In that case optimal land policies in (10) can be alternatively expressed simply as

$$\begin{aligned} \mathbf{c}_{it}^{lan}(\omega_{i,t-1}^{lan}, \rho_t) &= \frac{\alpha_i(1-\delta)\omega_{i,t-1}^{lan}(2+\rho_t)}{\alpha_i + \beta_i + \theta_i} \\ \mathbf{r}_{it}^{lan}(\omega_{i,t-1}^{lan}, \rho_t) &= \omega_{i,t-1}^{lan} - \frac{\theta_i(1-\delta)\omega_{i,t-1}^{lan}(2+\rho_t)}{\alpha_i + \beta_i + \theta_i}. \end{aligned} \tag{11}$$

Equation (11) displays the sensitivity of land use policies to changes in the land sink absorption rates.

3 Structure and Identification

The structural parameters in the production model are $\alpha_i, \beta_i, \gamma_i, \phi_i, \theta_i$, and the scale parameter, A_i. Ideally, these parameters could be estimated directly for each country. However, direct estimation of certain of the parameters is infeasible since existing carbon accounting methods do not distinguish between land consumption c_{it}^{lan}, land removals r_{it}^{lan}, and land sink s_{it}. All three are combined in measurements of *net* emissions from land after accounting for removals and sinks. However, only consumption (as measured by emissions) generates current production.

To get around these limitations, optimal land use policies in (10) are incorporated directly into the output equation (7) to produce a tractable "reduced form" equation in variables for which there is data. This yields the following equation system

expressed in natural logs:

$$Y_{it} = B_{i0} + B_{i1}X_{i1t} + B_{i2}X_{2it} + B_{i3}X_{3it} + \epsilon_{it} \tag{12}$$

where

$$Y_{it} = \log(y_{it}) \tag{13}$$

$$X_{it1} = \log\left(2\omega_{i,t-1}^{lan} + s_{it}^{lan}\right) \tag{14}$$

$$s_{it}^{lan} = \omega_{i,t-1}^{lan}\rho_t \tag{15}$$

$$X_{2it} = \log(c_{it}^{fos}) \tag{16}$$

$$X_{3it} = \log(L_{it}) \tag{17}$$

$$B_{i0} = \log(A_i) + \alpha_i \log\left(\frac{\alpha_i(1-\delta)}{\alpha_i + \beta_i + \theta_i}\right) + \beta_i \log\left(1 - \frac{(1-\delta)(\alpha_i + \theta_i)}{\alpha_i + \beta_i + \theta_i}\right) \tag{18}$$

$$B_{i1} = \alpha_i + \beta_i \tag{19}$$

$$B_{i2} = \gamma_i \tag{20}$$

$$B_{i3} = \phi_i \tag{21}$$

and

$$\epsilon_{it} = \log(\varepsilon_{i,t}) \tag{22}$$

In the equation system (12)-(22) the explanatory variable X_{1it} is a log composite of the country's one-period lagged carbon stock $\omega^{lan}_{i\,t-1}$ and its land sink s^{lan}_{it}. In turn, the country's land sink s^{lan}_{it} is a product of its lagged stock $\omega^{lan}_{i,t-1}$, and absorption rate ρ_t. The variables X_{2it} and X_{3it} are logs of L_{it} and c^{fos}_{it}, respectively.

Equation (15) follows from a simplifying assumption that the sequestration function F in Eq. (4) is the same for all countries. The country absorption rates can then computed from global absorption rates according to $s^{lan}_{it}/\omega^{lan}_{i,t-1} = \rho_t$ for each country i. Since ρ_t is observed directly, the functional form of F and the parameter vector π is not needed for the output estimation. These will be needed later on for the simulation exercise.

The "reduced form" parameters B_{i0}, B_{i1}, B_{i2} and B_{i3} are generated from structural parameters. Neither A_i nor θ_i are identified. These are largely nuisance parameters, however, as their role in the relationship between green house gas concentrations and GDP is fully summarized by the composite parameter B_{i0}. (Parameter θ_i is partially identified by the requirement that $\alpha_i + \beta_i + \theta_i > 0$.) More importantly, the production parameters α_i and β_i are only partially identified. Specifically, the sum $B_{i1} = \alpha_i + \beta_i$, but not the individual values of α_i and β_i, are identified. This follows from the fact that optimal policy responses c^{lan}_{it} and r^{lan}_{it} are collinear in the lagged stock $\omega^{lan}_{i,t-1}$. The other elasticities γ_i and ϕ_i are individually identified as B_{i2} and B_{i3}, resp.

The coefficient of interest is $B_{i1} = \alpha_i + \beta_i$. It approximates what we'll call the *policy-adjusted output elasticity* under optimal land use. The policy-adjusted elasticity is derived from the following terms. Let $y^*_i(\omega^{lan}_{i,t-1}, s^{lan}_{it})$ denote the optimized output when optimal land use policies $\mathbf{c}^{lan}_{it}(\omega^{lan}_{i,t-1}, s^{lan}_{it})$ and $\mathbf{r}^{lan}_{it}(\omega^{lan}_{i,t-1}, s^{lan}_{it})$ are in place. Carbon stock enters both as a direct input and as an indirect input via the optimal land use. The combination of the two in the log output equation yields

$$\begin{aligned}
&\alpha_i \log(\mathbf{c}^{lan}_{it}(\omega^{lan}_{i,t-1}, s^{lan}_{it})) \\
&+ \beta_i \log\left(w^{lan}_{i,t-1} - \mathbf{c}^{lan}_{it}(\omega^{lan}_{i,t-1}, s^{lan}_{it}) + \mathbf{r}^{lan}_{it}(\omega^{lan}_{i,t-1}, s^{lan}_{it})) + s^{lan}_{it}\right) \\
&\quad = (\alpha_i + \beta_i) \log(2\omega^{lan}_{i,t-1} + s^{lan}_{it}) = (\alpha_i + \beta_i) \log(\omega^{lan}_{i,t-1}(2 + \rho_t)) \equiv B_{i1} X_{i1t} \quad (23)
\end{aligned}$$

The last line in (23) follows from Equations (4) and (15). In this expression, the composition of shares in y^*_i into ecosystem and land consumption are described by the combined term $B_{i1}X_{i1t}$. From the term $B_{i1}X_{i1t}$, one derives the *policy-adjusted (output) elasticity* of the y^*_i with respect to lagged carbon stock ω^{lan}_{t-1}. The policy-adjusted elasticity, comprising a combination of direct and indirect changes in carbon

stock, is approximated by B_{i1}. Specifically,

$$\left(\frac{\partial y_i^*}{\partial \omega_{i,t-1}^{lan}}\right)\left(\frac{\omega_{i,t-1}^{lan}}{y_i^*(\omega_{i,t-1}^{lan}, s_{it}^{lan})}\right) \approx B_{i1} \equiv \alpha_i + \beta_i \tag{24}$$

Overall, land stocks are altered by carbon sink absorption and absorption rates are, in turn, altered due to GHG concentrations. B_{i1} then approximates the response in current output to increased GHGs.

4 Estimation

4.1 Overview

This section describes the data and estimation of the system (12)-(22). Subsection 4.2 describes the data. A complete description of the data sources and constructions are in Appendix. Subection 4.3 contains estimates for "reduced form" parameters corresponding to B_{i0}, B_{i1}, B_{i2} and B_{i3} in Equation (12).

To obtain a reasonable sample sizes, cross equation restrictions are imposed for countries with similar levels of development. Countries are clustered according to the U.N.'s Human Development Index (HDI) described below. As a robustness check, estimates are obtained for other clustering strategies.

In Section 5, these production estimates are combined with estimates of a land sink sequestration function that parsimoniously fits the data. The combination generates simulated time paths of land stocks and GDP over all clusters in the HDI.

4.2 The Data

The relevant times series are the country and global land stocks, $\{\omega_{it}^{lan}\}$ and $\{\omega_t^{lan}\}$, resp., the country and global land sinks $\{s_{it}^{lan}\}$ and $\{s_t^{lan}\}$, resp., the global GHG atmospheric stock $\{\omega_t^{atm}\}$, and the country-specific output, fossil fuel consumption, and labor force: $\{y_{it}\}$, $\{c_{it}^{fos}\}$ and $\{L_{it}\}$, respectively. Data for these time series spans 162 countries covering the time period 1990-2015.

Except for labor and GDP, units are measured in gigatonnes (Gt) of carbon dioxide equivalent (C02e) units. Units of C02e convert all green house gases into CO2 by measuring Global Warming Potential, a relative measure of how much heat a greenhouse gas traps in the atmosphere.[13] Labor is measured in size of workforce

[13]Definitions and all conversion factors are provided in the Appendix.

using standard definitions from the World Bank. GDP is measured in 2011 constant dollars.

The country land carbon stock series, $\{\omega_{it}^{lan}\}$, comes from FAOSTAT, the U.N. Food and Agricultural Organization's database which publishes updates of country data *every five years* based on U.N. reporting requirements that country data be reported at decadal and mid-decadal dates. From here on the dates t will range over the 5 year increments. i.e, $t = 1990, 1995, 2000, 2005, 2010, 2015$. This presents no problem for the theory since the model is agnostic about the length of a decision period. The notation "τ" will be used to represent annual time periods.

With this notation, the stock and flow data are as follows. Data on stocks $\{\omega_t, \omega_{it}^{lan}, \omega_t^{atm}, L_{it}\}$ are reported at quinquennial dates t. The data on flows are also reported at quinquennial dates t but represent aggregates over the past five years, up to and including the quinquennial date. Consequently, the flow data represented by a "tilde" on the variables are defined as

$$\tilde{s}_t^{lan} = \sum_{\tau=0}^{4} s_{t-\tau}^{lan}, \quad \tilde{c}_{it}^{fos} = \sum_{\tau=0}^{4} c_{t-\tau}^{fos}, \quad \tilde{y}_{it} = \sum_{\tau=0}^{4} y_{t-\tau} \tag{25}$$

for $t = 1990, 1995, 2000, \ldots, 2015$. In addition,

$$\tilde{\rho}_t \equiv \frac{\tilde{s}_t^{lan}}{\omega_{t-5}^{lan}} \quad \text{and} \quad \tilde{s}_{it}^{lan} = \omega_{i,t-5}^{lan}, \tilde{\rho}_t \tag{26}$$

are the quinquennial analogues of the earlier specification.

A quick summary of the variables, measurement units, and sources are listed in Table 1. These variables will those used to estimate the equation system (12)-(22). Details on units and sources are in Appendix 7.3.

Table 1: Summary of Data Variables.

Symbol	Units	Description	Source
ω_t^{lan}	Gt CO2e	Global carbon stock	Global Carbon Project
ω_{it}^{lan}	Gt CO2e	Country i carbon stock	FAOSTAT
ω_t^{atm}	Gt CO2e	Global GHG atmospheric stock	NOAA
L_{it}	population	Country i labor force	World Bank
$\tilde{s}_t^{lan}$	Gt CO2e	Global land sink over last 5 yrs	Global Carbon Project
$\tilde{s}_{it}^{lan}$	Gt CO2e	Country i land sink over last 5 yrs	calculated in Eq. (26)
$\tilde{c}_{it}^{fos}$	Gt CO2e	Country i fos. fuel emit. over last 5 yrs	World Resources Inst.
$\tilde{y}_{it}$	10^{12} 2011 dollars	Country i GDP over last 5 yrs	World Bank

All stocks are end-of-quinquennial time period. Variables with "tildes" are aggregates of annual flows over the five year year period up to and including the quinquennial year.

4.3 Production Parameter Estimates

We group countries using a standard measure, the United Nation's Human Development Index (HDI). The HDI formulates criteria for four distinct country groups: High Development, Medium High Development, Medium Low Development, or Low Development (United Nations Development Programme, 2019) The HDI partition to cluster countries allows for heterogeneous production according to different levels of development while also preserving reasonable sample sizes within each cluster.

The reduced form parameters B_{i1}, B_{i2} and B_{i3} are assumed identical across all countries within each development group. Under this cross-equation restriction, the estimating equation (27) reduces to

$$Y_{it} = B_{i0} + B_{k1}X_{i1t} + B_{k2}X_{2it} + B_{k3}X_{3it} + \epsilon_{kt} \tag{27}$$

for country i in HDI cluster k. Country-specific heterogeneity of the constant term B_{i0} is maintained using fixed effect dummies (via the scale term A_i).

Results are in Table 2. The main focus is on B_1 which, from Equation (24), is the policy-adjusted output elasticity of land stock. Strikingly, estimates for B_1 are statistically significant, as are all the coefficients, in the global cluster where all countries are included in the sample.[14]

The disaggregated estimates from the HDI partition indicate that the more precise estimates of B_1 come from the developed countries. Estimated $\hat{B}_1$ is larger and statistically significant for countries classified as High or Medium High development. It is not significant for the Medium Low or Low clusters. Significantly, the pattern is reversed for $\hat{B}_2$, the estimated value of the elasticity with respect to fossil fuels. $\hat{B}_2$ is not statistically significant for High development cluster but is for the others. Apparently, eco-capital rather than fossil fuels are associated with higher GDP growth for developed countries. Whereas, fossil fuels remain critical for less developed countries. The contrast between development groups plays a decisive role in the later simulations.

The policy adjusted elasticity definition in (24) is a useful guide for interpreting the estimates. The point estimates in Table 2 roughly approximate the incremental value of land carbon stock. Using the global cluster, a 1% increase (decrease) in global land carbon is associated with a roughly 0.36% increase (decrease) in annual GDP over the five year period following the change in carbon stock. The change in GDP includes the effects of both the increased (decreased) land consumption and the altered ecosystem.

[14] Unless otherwise stated, the references to statistically significance in the text refer to 1% levels.

Table 2: Estimated Policy-Adjusted Production Coefficients by Human Development Index Country Cluster.

	Dependent Variable - Log GDP				
Coefficients	High	Medium High	Medium Low	Low	All
B_1 Carbon Stock	0.759***	0.845***	0.004	0.057	0.385***
	(0.120)	(0.158)	(0.161)	(0.148)	(0.074)
B_2 Fossil Fuel	0.098	1.133***	1.045***	1.011***	0.963***
	(0.136)	(0.116)	(0.108)	(0.142)	(0.065)
B_3 Labor Force	0.561***	0.383***	0.713***	0.694***	0.631***
	(0.119)	(0.145)	(0.140)	(0.156)	(0.071)
Observations	230	225	180	175	810
R^2	0.995	0.995	0.996	0.994	0.995
F Statistic	562.4	578.9	658.7	423.8	626.6

OLS with Country-Fixed Effects. Standard errors in parentheses. Symbols *, **, and ** indicate statistically significant at the 10%, 5%, and 1% levels, respectively. Based on Human Development Index (HDI), U.N. Development Programme. #Observations = # countries in cluster × 5 quinquennial time periods, 1995-2015.

At a more disaggregated level, consider a country in the High development cluster. A 1% increase in its land carbon is associated with a 0.76% increase in its annual GDP, again over the next five year period. For the U.S. a conservative estimate for its five year GDP in the quinquennial period 2015-2020 is 93.36 trillion (2017 constant dollars). A 1% increase 2020 in carbon stock would result in an additional 623 billion USD over the 2020-25 period.[15] The observed increase in U.S. land carbon stocks from 2010 to 2015 was, in fact, around 1.5%. If this were to be replicated in the 2015-2020 period, then the increment to GDP would be about 1.3 trillion USD, or about 1.4% of GDP (averaging 0.28% increase in annual GDP) over the 2020-2025 period.

Of the increase in U.S. land carbon stock, almost a third of that was due to its land sink under the present methodology for calculating country sinks. Two thirds were due to reductions in land emissions and/or increases in removals. Consequently, any large reductions in land sink absorption rates over the next few decades could have substantial effects on growth rates, particularly for High and Medium High countries.

Applying the same logic for China, the observed increase in Chinese land carbon

[15]This is a rough estimate both because of B_1 approximates the actual elasticity in Eq. (24) and because it is an instantaneous rather than an interval elasticity).

from 2010-2015 was 6.7%. Applied to an estimated five year GDP of 61.2 trillion from 2015-2020, a 6.7% increase in land carbon stock from 2015-2020 produces an additional 3.46 trillion or 5.66% increase in GDP (using estimate from the Medium development cluster) over the 2020-2025 period.

As robustness check, several other partitions or *clustering strategies* are also considered. All told, we estimate the policy-adjusted output equation (27) for 8 clustering strategies: (i) the Global cluster (all 162 countries), (ii). the HDI clusters, (iii) binary HDI which groups High and Medium High together and Low and Medium together, (iv) binary inclusion/exclusion in the OECD, (v) binary inclusion/exclusion in top 30 GDP countries, (vi) binary inclusion/exclusion in top 30 GHG emitting countries, (vii) binary Inclusion/exclusion in the 35 most heavily forested countries as measured by carbon biomass, and finally (viii) regional partition into six clusters: North America, South and Central America (including Caribbean countries), Africa, Europe, Asia, and Oceana.[16]

The finer partitions allow for more cross-cluster heterogeneity; coarser partitions increase sample size within each cluster. The results for global and HDI clustering strategies (strategies (i) and (ii)) are in Table 2. The results for the other strategies are in the Appendix (Tables 5-10). In all the clustering strategies the estimates of B_1 are statistically significant for groupings that includes mostly developed countries — OECD membership, top GDP, top carbon emitters, etc. Cross-referencing the estimates in Table 2 with those from other Tables in the Appendix, the instances where estimated B_1 values are indistinguishable from zero tend to come from clusters consisting of highly forested countries in subsaharan Africa and Asia. The higher initial resource stock and lower level of development may have rendered these country's outputs less responsive to changes in the ecosystem thus far.[17]

5 Simulated Time Paths for 2020-2100

Estimates from the previous section are used here to simulate the model time paths for land carbon stocks and GDP over all country clusters. To run the simulations, we incorporate estimates from an parametric sequestration function in the next subsection. The simulations are then carried out under alternative concentration scenarios, each corresponding to one of the four standard *Representative Concentration Pathways (RCPs)* developed four research teams in the Global Carbon Project for IPCC's

[16] All data including membership lists for each clustering strategy are available upon request.

[17] The model does not address other ways in which developing countries may be vulnerable to climate change. See Althor, Watson, and Fuller (2016) and other references in the Introduction.

Fifth Assessment Report, 2014.

5.1 Sequestration Parameter Estimates

In order to simulate the time paths, models first requires an explicit, parametric form for the land sink sequestration function. The functional form should satisfy boundary conditions and the non-monotonicity posited earlier. The criteria are satisfied by a Gaussian land sink sequestration function expressed as

$$\log(\tilde{\rho}_t + 1) = \pi_0 + \pi_1 \omega_{t-5}^{atm} + \pi_2 (\omega_{t-5}^{atm})^2 + \eta_t \tag{28}$$

Recall that $\tilde{\rho}_t$ is the quinquennial sum of annual carbon land sink absorption rate defined in (4). If $\pi_2 < 0$ then the crucial property that sink absorption is an inverted-U function of concentrations is satisfied. In addition the unit adjustment to $\tilde{\rho}_t$ in the log term ensures that the lower bound condition, $\tilde{\rho}_t > -1$ is satisfied. Unlike a quadratic which falls rapidly after reaching a peak, the value of $\tilde{\rho}_t$ in (28) gradually declines and converges slowly to its lower bound. A mean zero random disturbance η_t reflects measurement error.

The estimated values $\hat{\pi}, \hat{\pi}_1, \hat{\pi}_2$ reported in Table 3 are consistent with the model. Figure 2 plots the land sink data against the fitted sequestration function.

Table 3: Estimated Coefficients of Land Sink Sequestration Equation (28).

π_0	π_1	π_2	R^2	F-stat
-0.500**	3.02E-4**	-4.19E-8**	0.485	12.7
(0.277)	(1.65E-4)	(2.44E-8)		

Standard errors in parentheses. Symbols *, **, and *** indicate statistically significant at the 10%, 5%, and 1% levels, respectivel

The negative coefficient π_2 provides support for inverted-U sequestration. It indicates that the global absorption rate reaches a maximum at atmospheric stock around $\omega_t^{atm} = 3650$ Gt CO2e (467.35 ppm CO2e) and declines thereafter. This is lower than peak CO2 absorption at constant temperatures, e.g. Xu (2015) and Thomson et al. (2008), suggesting that a warming climate plays a role.

The data suggests that climate change, apart from pure toxicity/nutrient effects from increased GHGs, contributes to reduced sink capacity.

The fitted global land carbon sequestration equation is displayed against sink rate data in Figure 2.

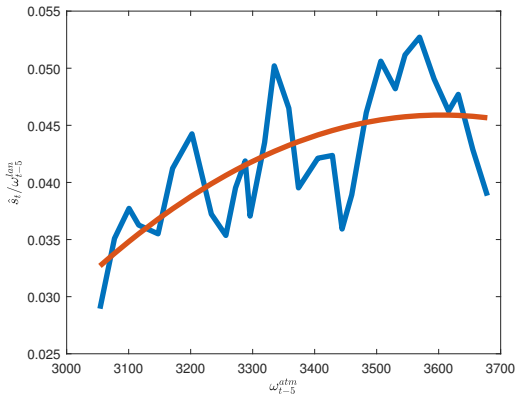

Figure 2: Fitted Sequestration Function Against Land-Sink Absorption Rate.

5.2 RCPs and Simulated Land Sink

A Representative Concentration Pathway (RCP) consists of various projected time paths for GHG emissions and concentrations. Each RCP corrresponds to a specific increase, either $+2.6, +4.5, +6.0$ or $+8.5$, in radiative forcing W/m^2 at the end of the 21st century relative to pre-industrial levels. Aggregating by region and sector, an RCP is based on a projected path of carbon factors (carbon per energy unit, kg C/GJ) and energy intensities (energy use per dollar income, GJ/\$) from the present to the end of the century. These projections are in turn generated by distinct integrated assessment models of energy use, fossil fuel emissions, mitigation investments, technological innovations. Lower carbon factor results from input substitution from high carbon emitting sources to lower ones. Lower energy intensity results from combination of technological innovation and conservation efforts.

A good overview is found van Vuuren et al. (2011)). The Appendix of our paper describes modeling assumptions and sources for each of the RCPs in more detail. Table 4 provides a rough summary.[18]

[18]See also van Vuuren et al. (2011), Fig 4).

Table 4: Summary of RCP Scenarios.

Scenario	Carbon Factor	Energy Intensity
RCP 2.6	Steepest decline	Steepest decline
	reaches lowest steady state	reaches lowest steady state
RCP 4.5	Moderate decline	Moderate decline
	reaches intermediate steady state	reaches intermediate steady state
RCP 6.0	Increase, peak, decline	Moderate decline
	reaches high steady state	reaches intermediate steady state
RCP 8.5	Constant	Slow decline
	remains at highest steady state	reaches highest steady state

The RCP 2.6 achieves the lowest concentrations scenario by 2100. It incorporates a carbon-limiting climate policy and higher rates rates of technological adoption. RCP 8.5 is the highest based on a business-as-usual setting.

Using RCP projections, we construct series on atmospheric stocks $\{\omega^{atm}_{t,RCP}\}$ and fossil fuel emissions $\{\tilde{c}^{fos}_{it,RCP}\}$ as t ranges over quinquennial dates from 2020-2100. The atmospheric series $\{\omega^{atm}_{t,RCP}\}$ are then fed into the estimated sequestration equation to produce land sink absorption rates which, in turn, are fed into the equilibrium law of motion to produce carbon stocks for 2020-2100. Finally, all the carbon stocks and flows are combined with a labor force forecast and fed into the estimated GDP equations to produce four GDP time paths for each country from 2020 to 2100.

The land sink absorption projections are displayed at the global level in Figure 3. It displays the calculation global sink absorption rate $\tilde{s}^{lan}_t/\omega^{lan}_{t-1}$ under each of four RCPs from 2020 onward. In three of the four scenarios, absorption ceases and turns negative by the end of the century. In these scenarios, CO2e atmospheric concentrations increase to the end of the century, albeit at decreasing rate for RCP 4.5. Negative values indicate a net *outflow* from land atmospheric carbon. The outflow can occur for a variety of reasons, including stresses from increasing or increasingly volatile temperature, destruction from severe weather events, and impediments to nutrient absorption for high enough CO2 concentrations (Hikosaka et al., 2006; Fernandez-Martinez et al., 2017; Raupach et al., 2014; Feng et al., 2015; Xu, 2015; Zheng et al., 2018). Only in the lowest emissions scenario RCP 2.6 does land sink increase. In this scenario, CO2e concentrations peak early and decline thereafter as strong carbon policies and mitigation technologies take effect. Significantly, the data on growth in GHG concentrations from to 2016 has outpaced the most severe scenarios posited in RCP 8.5.

The paths displayed are roughly consistent in shape though not in levels to fore-

casts of Thomson et al. (2008) who use the same RCP scenarios. The difference in levels is likely due to the fact that they measure both non-anthropogenic and anthropogenic (e.g., reforestation efforts) contributions to the land sinks. The latter utilizes forecasts of carbon pricing scenarios. Here we look at only non-anthropogenic sink capacity.

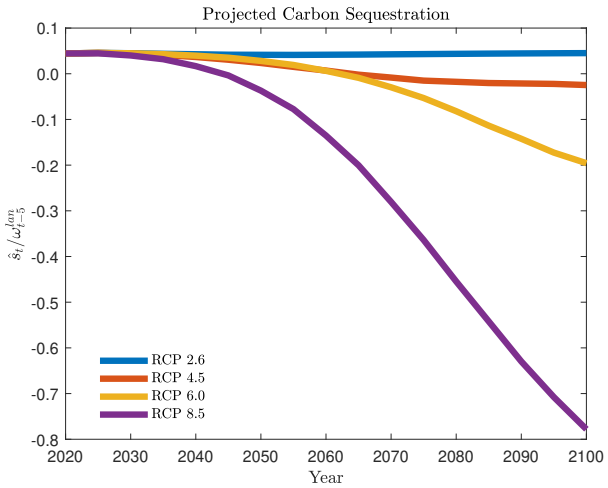

Figure 3: Projected Global Land Sink Absorption Rates, 2020-2100.

5.3 Simulations of Land Stocks and GDP

Using the estimates as calibrated parameters, we simulate the model for each of the four RCPs. Specifically, we simulate the dynamic paths of $\{\tilde{y}_{it,RCP}\}$, $\{\omega^{lan}_{it,RCP}\}$, and $\{\tilde{s}^{lan}_{it,RCP}\}$ $t = 2020, 2025, 2030, \ldots, 2100$ given the projected emissions $\{\omega^{atm}_{t,RCP}\}$, country hydrocarbon emissions $\{\tilde{c}^{fos}_{it,RCP}\}$ and labor force $\{L_{it}\}$.

The simulation fixes a given RCP forecast $\{\omega^{am}_{t,RCP}\}$ for atmospheric stocks. It then produces model generated series for land stocks and GDP as follows: Step (i): construct the predicted global land sink absorption series $\left\{\frac{\widetilde{s^{lan}_{t,RCP}}}{\omega^{lan}_{t-1,RCP}}\right\}$ from the land sink estimation given parameter estimates $\hat{\pi}_0$, $\hat{\pi}_1$, and $\hat{\pi}_2$; Step (ii): recursively generate the series for land stocks $\{\omega^{lan}_{it}\}$ from the model law of motion under estimated parameters in optimal land policy; Step (iii): generate GDP from the predicted value of given $\hat{B}_{i0}, \hat{B}_{i1}, \hat{B}_{i2}$ and $\hat{B}_{i3}$ and given exogenously constructed series for labor $\{L_{it}\}$ and fossil fuel emissions $\{\tilde{c}^{fos}_{it}\}$. The complete algorithm is detailed in the Appendix.

Since the optimal land use parameters in the estimation stage are not fully identified, the algorithm does not generate direct projections on future land use. Conse-

quently, the consistency of the model with land use scenarios in the RCPs themselves cannot be verified.[19]

The results of Step (ii), the simulation of land carbon stocks for each cluster and each RCP, are displayed in Figure 4. The graphs in the Figure display the four RCP time paths together in each of the four HDI clusters. An alternative display of graphs organized by RCP scenarios is in Figure 11 in the Appendix.

Not surprisingly, low concentration scenarios RCP 2.6 and 4.5 display higher stocks through time than the higher concentration scenarios 6.0 an 8.5. RCP 2.6, which corresponding to the lowest emissions and most aggressive mitigation policies, displays the most growth in land carbon stocks regardless of the particular development cluster.

After mid-century, the differences between the lower and higher emissions scenarios display starkly different environmental outcomes particularly in High and Medium High clusters. Moreover, in the High and Medium High clusters, the stocks increase in low concentration scenarios while in Medium Low and Low countries, the stocks decline in every scenario. This may be because mitigation technologies and more sustainable land policies are already in use in the more highly developed countries.

[19]In principle, the global balance equation could be used to to generate CO2e emissions from optimal land use in the model. To proceed, one would need to include a full model of ocean sinks, well beyond the scope of the exercise.

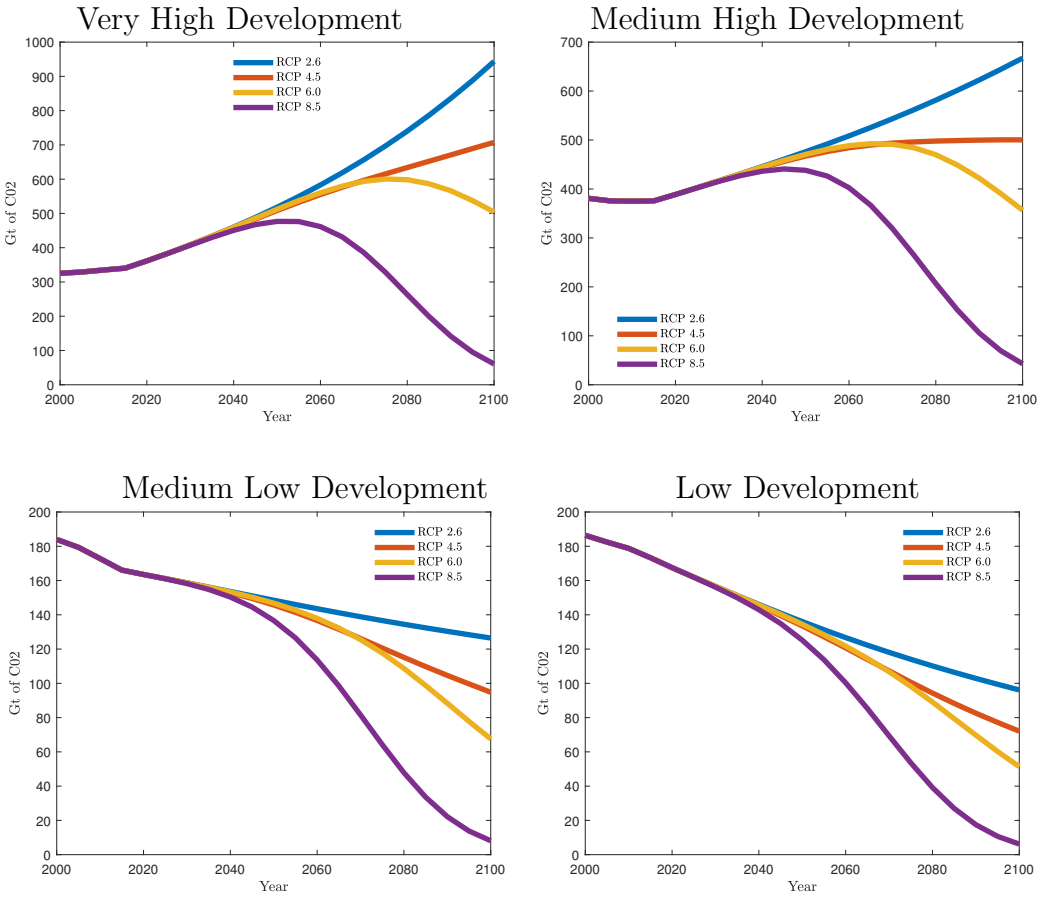

Figure 4: Land Carbon Stocks by HDI Cluster.

The growth paths shown Figure 4 are comparable to net land emissions in Thomson et al. (2008). They use an IAM framework similar to the one use in RCP 4.5 in order to estimate total yearly anthropogenic sequestration. Their paths resemble ours for High Development countries under the intermediate scenario RCP 6.0.

The final step in the exercise simulates GDP to the end of the century in each RCP scenario, for each country, and for each cluster. The results are displayed in Figure 5, again displaying the four RCP time paths in each of the four HDI clusters (as with Figure 4). An alternative display by RCP scenarios is in Figure 12 in the Appendix.

Three of the four clusters display a natural ordering of the scenarios by the end of the century. For the High development cluster, GDP growth is higher the lower the concentrations/emissions scenario. For the Low and Medium Low clusters, the

pattern is reversed: GDP growth is higher the higher the concentration scenario. For the Medium High development cluster, the intermediate scenarios are most growth enhancing.

Significantly, both High and Medium High development clusters show a display a "peak and decline" pattern in GDP for the two highest concentration scenarios 8.5 and 6.0. Under RCP 8.5, GDP in the High development cluster grows at an annual rate of 1% until mid-century, after which time it falls at a dramatic 10% per annum.

In other words, high emissions scenarios appear catastrophic for highly developed countries. This may seem unlikely. The decline is largely driven by two factors: the collapse in land carbon stock due to dramatic declines in sink absorption rates, and the lack of innovation in mitigation technology - a built in feature of the 8.5 RCP scenario.

RCPs 4.5 and 2.6, by contrast, assume mitigation improvements and earlier peaks in fossil fuel use. These scenarios are supported by Mohr et al. (2015) who provide estimates of fossil fuel extraction costs that suggest the lower scenarios may more likely. In our simulations, growth in highly developed countries' GDP in low concentration scenarios continues after mid-century. Under scenario RCP 2.6, growth in the High Development cluster averages 0.8% per year. This is somewhat lower than the recent trend but not out of line with forecasts of declining population growth highly developed countries. Countries with higher projected population growths are likely to experience higher growth than 0.8% average for this cluster.

The simulations suggest then that the low concentration scenario displays the best prospects for long run GDP growth among the developed nations. For these countries, the declining influence of fossil fuels together with the large influence of eco-capital (as shown in table 2) makes the low emission scenario most attractive among the four.

By contrast, GDP growth declines or is flat under RCP 2.6 in all other clusters. The Low development cluster, in particular performs well under RCP 8.5 averaging around 2.5% annual growth. For countries in this cluster, land carbon matters less than fossil fuel-driven growth.

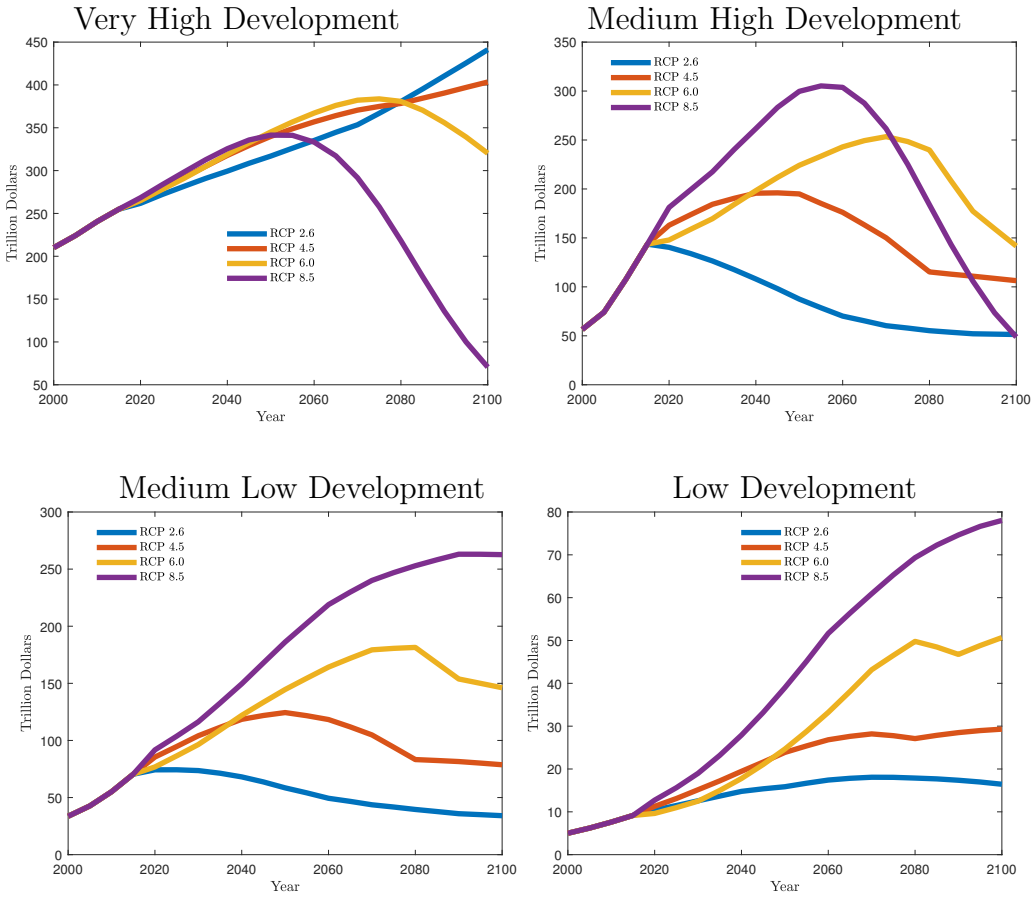

Figure 5: Quinquennially Aggregated GDP by HDI Cluster.

The global picture is summarized in Figure 6. The Figure displays the aggregation of GDP across all four HDI clustered groups. Figure 6 shows that by the end of the century the moderate-to-high scenario 6.0 produces the most growth. By appearances, however, the path trend is decreasing for 6.0 and increasing for 4.5 and 2.6. Hence, if the paths continued into the 22nd century according to trend then GDP under RCP 6.0 would probably be overtaken by the low-intermediate scenario RCP 4.5, and possibly even the lowest scenario RCP 2.6.

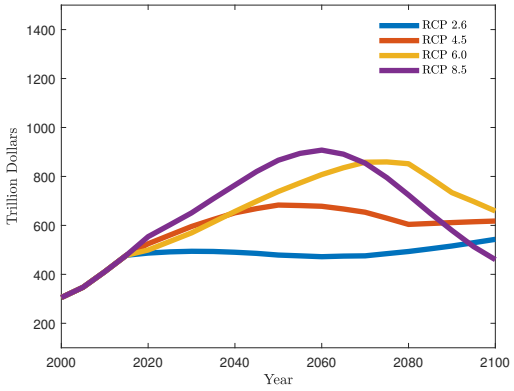

Figure 6: Global GDP, Aggregated Quinquennially and Across HDI Clusters.

If the trend in Figure 6 holds up, it suggests again that the best-case prospect for growth requires some form of transfer from the highly developed countries to lower developed ones. This would be necessary even if the high-intermediate scenario 6.0 remains the best-case. Current emissions trajectories are exceeding even the original RCP 8.5 scenario.

The results also point to the drawbacks of seemingly straightforward solutions such as technological transfers. Such transfers are intended to place production technologies of developed nations into the hands of developing ones. In fact, this would produce lower growth for these countries than under their current technologies, assuming optimal land use adjustments by these countries. In other words, technology transfer may be a poor substitute for direct aid.

Finally, we note that the path contours in Figure 6 are not specific to the HDI cluster strategy. The simulations were run under all eight cluster strategies. A side-side comparison of all eight is displayed in Figure 13 in the Appendix and reveals only minor differences.

5.4 Isolating the Effects of the Land Sink Mechanism

The land sink mechanism, whereby increased GHG concentrations eventually deteriorate sink absorption, plays a role in the simulation results. How big a role does it play?

To address the question, we perform a simple counterfactual experiment. We simulate a version of the model in which the land sink absorption rate is held fixed at its empirical average value $\rho = .043$ Gt CO2e over the sample period (Figure 7). Everything else is the same as before. We refer to this as the "constant sink model" and compare it with the "active sink (inverted U) model".

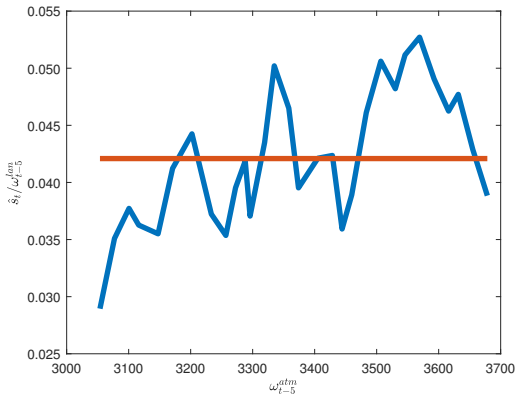

Figure 7: Counterfactual Constant Sequestration.

The resulting time paths are displayed in Figures 8-10. Figure 8 displays RCP paths of carbon land stocks in each cluster in the constant sink model. By keeping land sink absorption constant, the paths are *entirely driven* by simulated forecasts of land use practices. Carbon stocks therefore do not vary over RCP scenarios. The Figure shows that intensive deforestation in the low development countries leads to declines in land stocks. Increased reforestation in high development countries leads to increases in stocks.

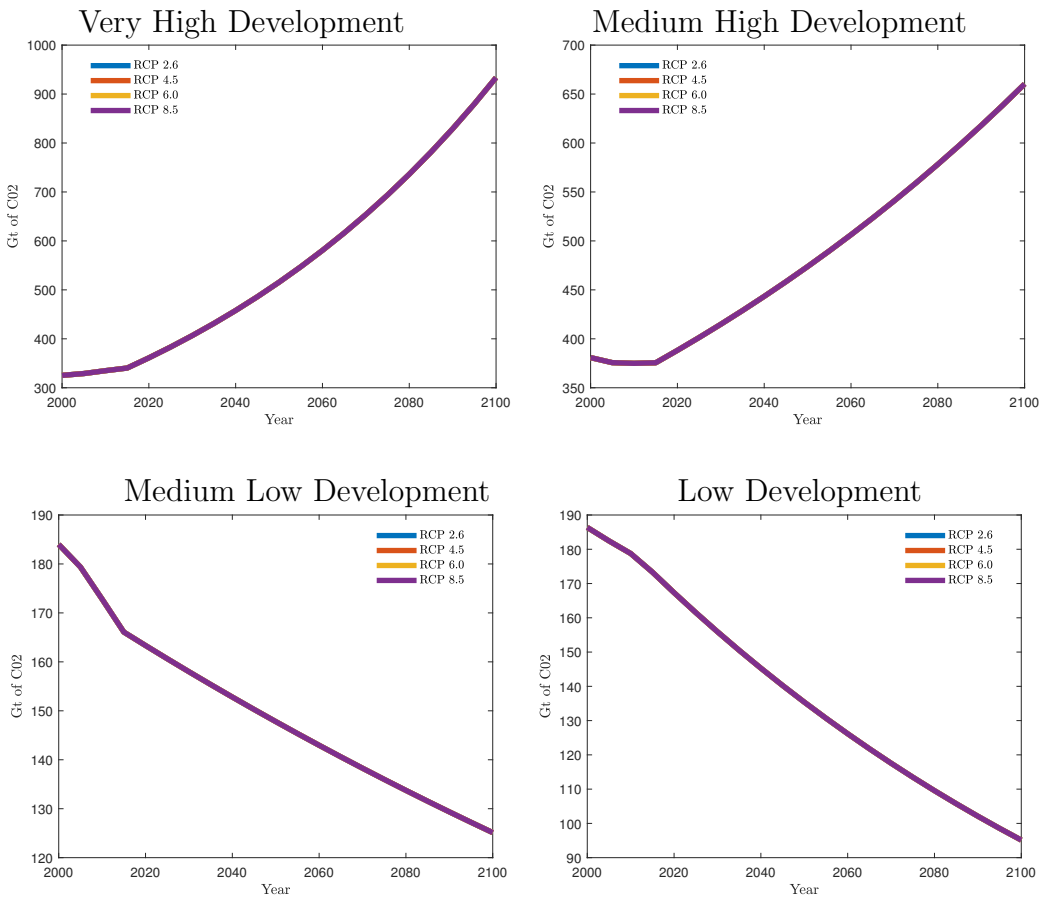

Figure 8: Land Carbon Stocks by HDI Cluster in Constant Sink Model.

Yet, in stark contrast with the active land sink model, the highest emissions/concentrations scenarios are most conducive to GDP growth in all four clusters. This is displayed in Figure 9. Growth rates range from 1% in the High development cluster to 2.4% in the Low development cluster.

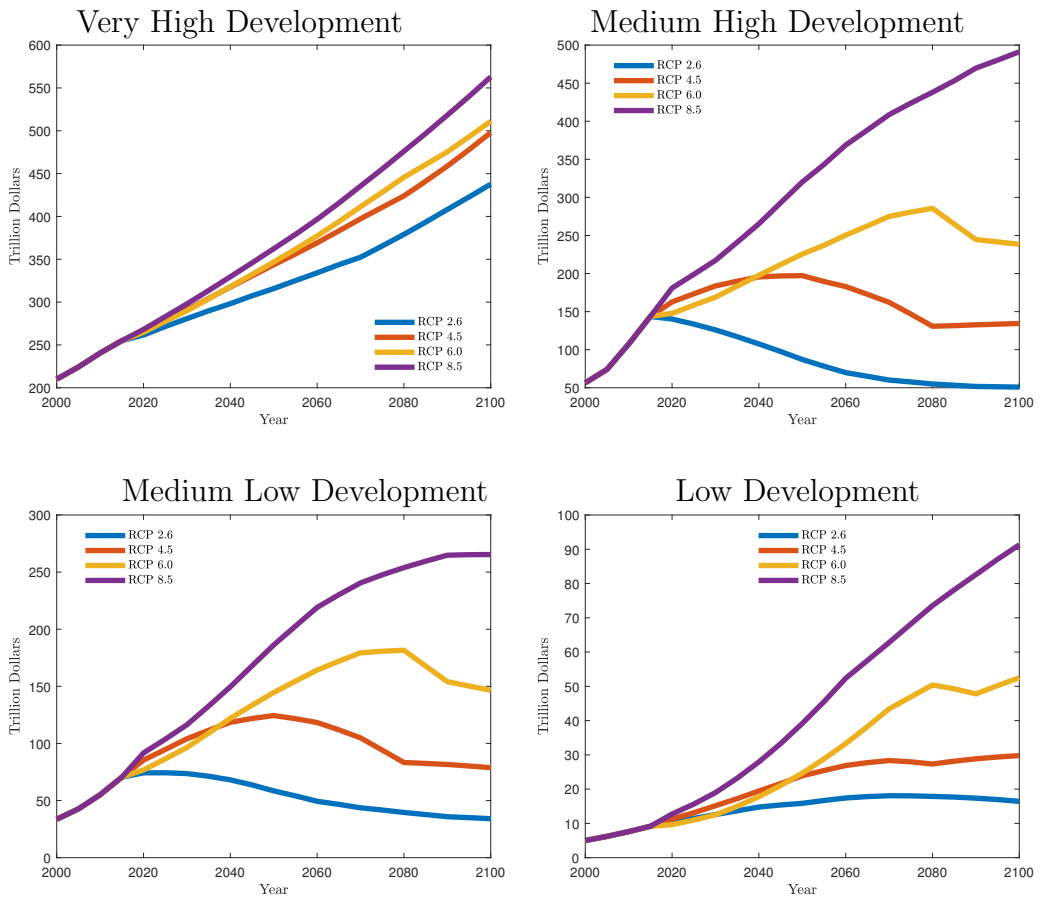

Figure 9: Quinquennially Aggregated GDP by HDI Cluster in Constant Sink Model.

In all cases, the best-case scenario in the constant sink model produces higher growth rates than the best-case scenario in the active sink model. This fact is not surprising since the active sink model shows declines in the absorption rate by 2020 in high concentrations scenarios but not low ones. What is striking is how large the differences between the two models are. These differences are displayed in Figure 10. Figure 10 displays side-by-side the simulated global GDPs in both the active and constant sink models. In the constant sink model, the ordering of the scenarios from high to low concentrations is maintained throughout. Unlike the active sink model, there are no reversals or sharp declines.

In a comparison of best-case scenarios, annual GDP growth in both models are comparable (under RCP 8.5) until mid-century at which point they diverge sharply. Annual global GDP growth in the active sink model in the best-case is 0.28% by

2100. Increases up to 2060 are largely offset by decreases thereafter. Whereas, annual GDP growth to 2100 in the constant model in the best-case is 1.5% annually under the constant sink model. Initially large increases taper off later in the century. This is roughly in line with long run projections by the Organisation for Economic Co-operation and Development (Organisation for Economic Co-operation and Development, 2019), none of which incorporate active land sinks. To put the sink model comparison in perspective, by the end of the century global output under active sink rate is less than a third of what it would be in the absence of a decreasing sink.

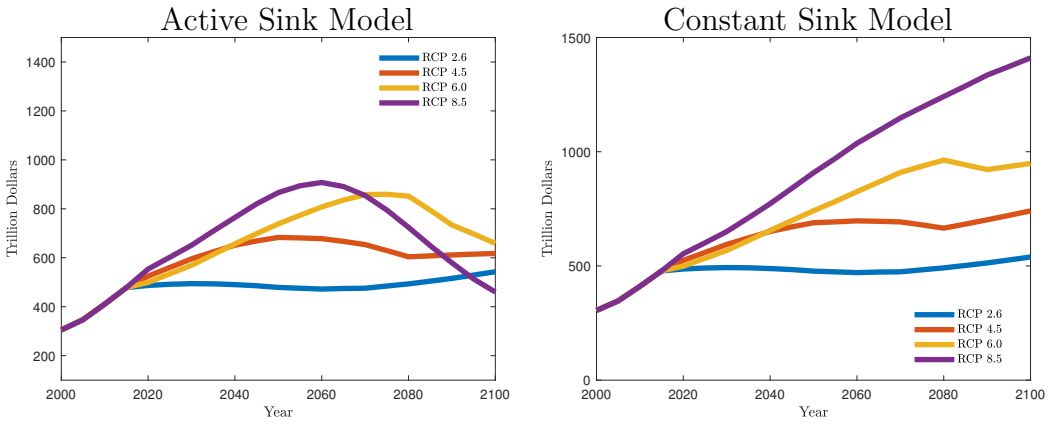

Figure 10: Active vs Constant Sink Comparison: Global GDP, Aggregated Quinquennially and Across HDI Clusters.

6 Concluding Remarks

All IAMs trade-off richness with tractability. The present paper leans toward the latter, omitting details on the energy sectors. This allows us to isolate effects of one causal mechanism: land sink sequestration. It is one among many mechanisms that determine damage from climate change. Even so, the mechanism is subtle. The effects of GHG concentrations on output work both directly and indirectly via endogenous land use.

Estimated coefficients show that terrestrial carbon stocks, adjusted for optimal land use, have potentially large effects on GDP growth, particularly in more highly developed countries. It is unclear why the GDPs of developed countries, more so than others, would be more responsive to land stock changes. One possibility is that interdependencies in more advanced technologies, e.g., computerization of wastewater management systems, are increasingly sensitive to small changes in the ecosystem.

The simulation make use of the estimated sequestration function. In physiological terms, sink rates are already shown to be sensitive to CO2 concentrations. High concentrations of GHGs are shown to diminish sinks. Fitting the land sink to a Gaussian sequestration function, we apply the model and production estimates to the standard RCP scenarios.

The simulation results display widely divergent trajectories between developing and developed countries. Developed countries do well under low concentration scenarios. This may be because mitigation and conservation techniques that lower production shares in fossil fuels have already been widely adopted. Less developed countries, by contrast, do badly in low emissions scenarios and better in high emissions scenarios (at least until 2100). A larger production share in those countries comes from fossil fuels.

Finally, the counterfactual simulations under constant land sink suggest then that long run prospects for GDP growth appear highly sensitive to environmental responses to GHG concentrations.

A few caveats are necessary. First, the simulations are based on a fitted sequestration function. External validation exists for some, but not all, of its attributes. A different approach is taken by Lubowski, Plantinga, and Stavins (2005) who study anthropogenic removals in an econometric model of land use and sinks. Their approach rules out non-monotone sequestration since sinks are calculated from removals using standard conversion tables (Birdsey, 1992). Their approach is closer to the constant sink model we analyze earlier. The studies that validate the active land sink model are typically localized or take place in controlled environments. Less is known about the back end of this relationship if or when CO2 concentrations reach unprecedented levels. This is most relevant for RCP 8.5 scenario in which concentration levels almost triple by 2100.

Second, the simulation model is calibrated to the elasticity estimates over the 1990-2015 period. Hence, we only project out from current technological trends. The simulation nevertheless establishes an important baseline for future global policies, particularly as they address the divergent outcomes across developed and developing countries in the RCP scenarios.

Third, there is, as one might expect, considerable controversy about the RCP scenarios. Some claim that RCP 2.6 is all but impossible since the realized path of GHGs has exceeded 2.6 by a wide margin since the scenario was initially published. Others claim that the highest scenario, RCP 8.5, is too extreme to be considered a "business-as-usual" scenario. The present study makes no claim about which, if any, is most likely. By design it utilizes all four. Our intention to present a broad collection of "possible futures" as a way to facilitate comparisons both across

countries and across time.

Fourth, our study makes projections based on a single model with many limitations outlined in the previous section. Climate uncertainty will produce a wide quantitative variation across different models, of which ours is only a small part (Burke, Hsiang, and Miguel, 2015). In our view this calls for caution in interpretation rather than rejection of single-model studies. As with economic modeling generally, we find a substantial upside in working with a specific IAM that highlights a few key features — in our case land sink — among the many that determine climate costs. Our purpose is to isolate incentives and trade offs faced by policymakers that may be obfuscated when aggregating forecasts across highly differentiated models.

Finally, the present study focuses exclusively on GDP, a flawed indicator of climate costs. The high growth in output resulting from high emissions scenarios may, in fact, be consistent with poor socio-economic indicators such as lower life expectancy, wellness, and leisure, and increases in congestion, population density, and crime. Even in the context of the model, comparisons are about GDP rather than payoffs. This simplifies the simulation strategy; deterministic simulations can be used since shocks enter additively into GDP and wash out in expectation. However, in terms of welfare the volatility of shocks matter a great deal to a representative citizen who values consumption smoothing. In welfare calculations, stochastic simulations that aggregate across payoff paths provide a better indication of true trade offs within the model. Future work to incorporate broad measures of well being into climate cost scenarios are well worth the effort.

References

Acemoglu, D., P. Aghion, L. Bursztyn, and D. Hemous. 2012. "The Environment and Directed Technical Change." *American Economic Review* 102(1):131–166.

Althor, G., J. Watson, and R. Fuller. 2016. "Global Mismatch between Greenhouse Gas Emissions and the Burden of Climate Change." *Scientific Reports* 6(20281).

Birdsey, R.A. 1992. "Carbon Storage and Accumulation in United States Forest Ecosystems." General Technical Report WO-59, U.S.D.A., Forest Service, Washington, DC.

British Petroleum. 2019. "Statistical Review of World Energy." Accessible at www.bp.com.

Burke, M., S.M. Hsiang, and E. Miguel. 2015. "Global Non-Linear Effect of Temperature on Economic Production." *Nature* 527:235–39.

Cai, Y., K. Judd, T. Lenton, T. Lontzek, and D. Narita. 2015. "Environmental Tipping Points Significantly Affect the Cost-Benefit Assessment of Climate Policies." *Proceedings of the National Academy of Sciences of the United States of America* 112(15):4606–4611.

Cai, Y., K. Judd, and T. Lontzek. 2012. "Tipping Points in a Dynamic Stochastic IAM." Working Paper 12-13, Robust Decision-making on Climate and Energy Policy, Chicago, IL.

Canadell, J., C. Le Quere, M. Raupach, C. Field, E. Buitenhuis, P. Ciais, T. Conway, N. Gillett, R. A. Houghton, and G. Marland. 2007. "Contributions to Accelerating Atmospheric CO2 Growth from Economic Activity, Carbon Intensity, and Efficiency of Natural Sinks." *Proceedings of the National Academy of Sciences of the United States of America* 104(47):18866–18870.

Cave, J. 1987. "Long-Term Competition in a Dynamic Game: The Cold Fish War." *Rand Journal* 18(4):596–610.

Clarke, L., J. Edmonds, H. Jacoby, H. Pitcher, J. Reilly, and R. Richels. 2007. "Scenarios of Greenhouse Gas Emissions and Atmospheric Concentrations." Tech. rep., U.S. Climate Change Science Program and the Subcommittee on Global Change Research. Department of Energy, Office of Biological and Environmental Research, Washington, DC.

Dell, M., B. Jones, and B. Olken. 2012. "Temperature Shocks and Economic Growth: Evidence from the Last Half Century." *American Economic Journal: Macroeconomics* 4(3):66–95.

Deryugina, T. and S. Hsiang. 2017. "The Marginal Product of Climate." Working Paper 24072, National Bureau of Economic Research, Cambridge, MA.

Dutta, P. and R. Radner. 2004. "Self-Enforcing Climate-Change Treaties." *Proceedings of the National Academy of Sciences of the United States of America* 101(14):5174–5179.

———. 2006. "A Game-Theoretic Approach to Global Warming." In *Advances in Mathematical Economics, Volume 8*, edited by S. Kusuoka and A. Yamazaki. Tokyo, Japan: Springer, 135–153.

———. 2009. "A Strategic Analysis of Global Warming: Theory and Some Numbers." *Journal of Economic Behavior and Organization* 71(2):187–209.

FAO. 2015. "Forest Resources Assessment." Report, Food and Agricultural Organization of the United Nations, Rome, Italy.

———. 2019. "FAOSTAT." Accessible at www.fao.org/faostat/en/.

Feng, Z., T. Rutting, H. Pleijel, G. Wallin, P. Reich, C. Kamnann, P. Newton, K. Kobayashi, Y. Luo, and J. Udding. 2015. "Constraints to Nitrogen Acquisition of Terrestrial Plants under Elevated CO2." *Global Change Biology* 21(8):3152–3168.

Fernandez-Martinez, M., S. Vicca, I. Janssens, P. Ciais, M. Obersteiner, M. Bartrons, J. Sardans, A. Verger, J.G. Canadell, F. Chevallier, X. Wang, C. Bernhofer, P.S. Curtis, D. Gianelle, T. Grünwald, B. Heinesch, A. Ibrom, A. Knohl, T. Laurila, B. Law, J. Limousin, B. Longdoz, D. Loustau, I. Mammarella, G. Matteucci, R. Monson, L. Montagnani, E. Moors, J. Munger, D. Papale, S. Piao, and J. Pe nuelas. 2017. "Atmospheric Deposition, CO2, and Change in the Land Carbon Sink." *Scientific Reports* 7(1):9632.

Fisher, R. and L. Mirman. 1992. "Strategic Dynamic Interactions: Fish Wars." *Journal of Economic Dynamics and Control* 16(2):267–287.

Fujino, J., R. Nair, M. Kainuma, T. Masui, and Y. Matsuoka. 2006. "Multi-Gas Mitigation Analysis on Stabilization Scenarios Using AIM Global Model: Multigas Mitigation and Climate Policy." *The Energy Journal* 27(3):343–354.

Golosov, M., J. Hassler, P. Krusell, and A. Tsyvinski. 2014. "Optimal Taxes on Fossil Fuel in General Equilibrium." *Econometrica* 82(1):41–88.

Harrison, R. and R. Lagunoff. 2017. "Dynamic Mechanism Design for a Global Commons." *International Economic Review* 58(3):751–782.

———. 2019. "Tipping Points and Business-as-Usual in a Global Commons." *Journal of Economic Behavior and Organization* 163(July):386–408.

Hijioka, Y., Y. Matsuoka, H. Nishimoto, M. Masui, and M. Kainuma. 2008. "Global GHG Concentration Scenarios under GHG Concentration Stabilization Targets." *Journal of Global Environmental Engineering* 13:97–108.

Hikosaka, K., I. Kazumasa, A. Borjigidai, O. Muller, and Y. Onoda. 2006. "Temperature Acclimation of Photosynthesis: Mechanisms Involved in the Changes in Temperature Dependence of Photosynthetic Rate." *Journal of Experimental Botany* 57(2):291–302.

Hsiang, S., R. Kopp, A. Jina, J. Rising, M. Delgado, S. Mohan, D.J. Rasmussen, R. Muir-Wood, P. Wilson, M. Oppenheimer, K. Larsen, and T. Houser. 2017. "Estimating Economic Damage from Climate Change in the United States." *Science* 356(6345):1362–1369.

IPCC. 2014. "Fifth Assessment Report on Climate Change." Technical report, Inter-Governmental Panel on Climate Change, Geneva, Switzerland.

Ito, A.J., M. Penner, C. Prather, C. de Campos, R.A. Houghton, T. Kato, A. Jain, X. Yang, G. Hurtt, S. Frolking, M. Fearon, L. Chini, A. Wang, and D. Price. 2008. "Can We Reconcile Differences in Estimates of Carbon Fluxes from Land-Use Change and Forestry for the 1990s?" *Atmospheric Chemistry and Physics* 8(12):32913310.

Krusell, P. and A. Smith. 2009. "Macroeconomics and Global Climate Change: Transition for a Many-Region Economy." Working paper, Institute for International Economic Studies and Princeton University, Princeton, NJ.

Le Quere, C., R. Andrew, R. M., Friedlingstein, P., Sitch, S., Hauck, J., Pongratz, J., Pickers, P. A., Korsbakken, J. I., Peters, G. P., Canadell, J. G., Arneth, A., Arora, V. K., Barbero, L., Bastos, A., Bopp, L., Chevallier, F., Chini, L. P., Ciais, P., Doney, S. C., Gkritzalis, T., Goll, D. S., Harris, I., Haverd, V., Hoffman, F. M., Hoppema, M., Houghton, R. A., Hurtt, G., Ilyina, T., Jain, A. K., Johannessen, T., Jones, C. D., Kato, E., Keeling, R. F., Goldewijk, K. K., Landschützer, P., Lefèvre, N., Lienert, S., Liu, Z., Lombardozzi, D., Metzl, N., Munro, D. R., Nabel, J. E. M. S., Nakaoka, S.-I., Neill, C., Olsen, A., Ono, T., Patra, P., Peregon, A., Peters, W., Peylin, P., Pfeil, B., Pierrot, D., Poulter, B., Rehder, G., Resplandy, L., Robertson, E., Rocher, M., Rödenbeck, C., Schuster, U., Schwinger, J., Séférian, R., Skjelvan, I., Steinhoff, T., Sutton, A., Tans, P. P., Tian, H., Tilbrook, B., Tubiello, F. N., van der Laan-Luijkx, I. T., van der Werf, G. R., Viovy, N., Walker, A. P., Wiltshire, A. J., Wright, R., Zaehle, S., Zheng, and B. 2018. "Global Carbon Budget 2018." *Earth Systems Science Data* 10(4):2141–2194.

Levhari, D. and L. Mirman. 1980. "The Great Fish War: An Example Using a Dynamic Cournot-Nash Solution." *Bell Journal of Economics* 14(1):322–334.

Lubowski, R.N., A Plantinga, and R. Stavins. 2005. "Land-Use Change and Carbon Sinks: Econometric Estimation of the Carbon Sequestration Supply Function." *Journal of Environmental Economics and Management* 51(2):135–152.

Mcalpine, K.G. and D.M. Wotton. 2009. "Conservation and the Delivery of Ecosystem Services: A Literature Review." Science for Conversation Report 295, New Zealand Department of Conservation, Wellington, New Zealand.

Mohr, S., J. Wang, G. Ellem, J. Ward, and D. Giurco. 2015. "Projection of World Fossil Fuels by Country." *Fuel* 141(1):120–135.

Mooney, C. and Z. Murphy. 2019. "Gone in a Generation."

Narayan, S., M. Beck, P. Wilson, C. Thomas, A. Guerrero, C. Shepard, B. Reguero, G. Franco, J. Ingram, and D. Trespalacios. 2017. "The Value of Coastal Wetlands for Flood Reduction in the Northeastern USA." *Scientific Reports* 7(1):9643.

Nordhaus, W. 2013. "Integrated Economic and Climate Modeling." In *Handbook of Computable General Equilibrium Modeling, Volume 1*, edited by P. B. Dixon and D. Jorgenson. Amsterdam, The Netherlands: Elsevier, 1069–1131.

———. 2018. "Projections and Uncertainties about Climate Change in an Era of Minimal Climate Policies." *American Economic Journal: Economic Policy* 10(3):333–360.

Organisation for Economic Co-operation and Development. 2019. "The Long View: Scenarios for the World Economy to 2060." Accessible at www.oecd.org. Accessed July 29, 2019.

Power, A. 2010. "Ecosystem Services and Agriculture: Tradeoffs and Synergies." *Philosophical Transactions of the Royal Society B* 365(1554):2959–2571.

Raupach, M.R., M. Gloor, J.L. Sarmiento, J.G. Canadell, T.L. Fralicher, T. Gasser, R.A. Houghton, C. Le Quere, and C.M. Trudinger. 2014. "The Declining Uptake Rate of Atmospheric CO2 by Land and Ocean Sinks." *Biogeosciences* 11(13):3453–3475.

Riahi, K. and N. Nakicenovic. 2007. "Greenhouse Gases - Integrated Assessment." *Technological Forecasting and Social Change* 74(7):873–1108.

Rights and Resources Initiative. 2015. "Who Owns the World's Land? A Global Baseline of Normally Recognized Indigenous and Community Land Rights." Tech. rep., Rights and Resources Group, Washington, DC.

Thomson, A., R. Izaurralde, S. Smith, and L. Clarke. 2008. "Integrated Estimates of Global Terrestrial Carbon Sequestration." *Global Environmental Change* 18(1):192–203.

United Nations Development Programme. 2019. "Human Development Reports." Accessible at www.hdr.undp.org.

van Vuuren, D.P., M. den Elzen, P. Lucas, B. Eickhout, B. Strengers, B. van Ruijven, and S. Wonink andand R. van Houdt. 2007. "Stabilizing Greenhouse Gas Concentrations At Low Levels: An Assessment of Reduction Strategies and Costs." *Climatic Change* 81(2):119–159.

van Vuuren, D.P., J. Edmonds, M. Kainuma, K. Riahi, A. Thomson, K. Hibbard, G.C. Hurtt, T. Kram, V. Krey, J.F. Lemarque, T. Matsui, M. Meinhausen, N. Nakicenovic, S. Smith, and A. Rose. 2011. "The Representative Concentration Pathways: an Overview." *Climatic Change* 109(1):5–31.

van Vuuren, D.P., B. Eickhout, P.L. Lucas, and M.G.J. den Elzen. 2006. "Long-Term Multi-Gas Scenarios To Stabilise Radiative Forcing — Exploring Costs and Benefits within an Integrated Assessment Framework: Multigas Mitigation and Climate Policy." *The Energy Journal* 27(1):201–234.

Vincent, C.H., L.A. Hanson, and C.N. Argueta. 2017. "Federal Land Ownership: Overview and Data." Tech. rep., Congressional Research Service, Washington, DC.

Wise, M.A., K.V. Calvin, A.M. Thomson, L.E. Clarke, B. Bond-Lamberty, R.D. Sands, S.J. Smith, A.C. Janetos, and J.A. Edmonds. 2009. "Implications of Limiting CO2 Concentrations for Land Use and Energy." *Science* 324(5931):1183–1186.

Xu, M.N. 2015. "The Optimal Atmospheric CO2 Concentration for the Growth of Winter Wheat (Triticum Aestivum)." *Journal of Plant Physiology* 184(July):89–97.

Zheng, Y., F. Li, A.A. Shedayi, L. Guo, C. Ma, B. Huang, and M. Xu. 2018. "The Optimal CO2 Concentrations for the Growth of Three Grass Species." *BMC Plant Biology* 18(1):27.

Zomer, R.J., H. Neufeldt, J. Xu, A. Ahrends, D. Bossio, A. Trabucco, M. van Noordwijk, and M. Wang. 2016. "Global Tree Cover and Biomass Carbon on Agricultural Land: The Contribution of Agroforestry to Global and National Carbon Budgets." *Scientific Reports* 6:29987.

7 Appendix

7.1 Derivation of the Optimal Land Use Policies

Due to additively separability under log payoffs, we can drop the noise term ϵ_{yit} and the terms c_{it}^{fos} and L_{it} from the derivation of optimal land policy for country i. None of these terms enter into i's policy function.

Consequently, we also drop the "lan" superscript and the country subscript " i" from land consumption c_{it}^{lan}, removals r_{it}^{lan}, land stock ω_{it}^{lan}, and land sink s_{it}^{lan}.

Dropping these terms, the structural equations are expressed as

$$u_t = \log(y_t) + \theta \log(\omega_{t-1} - r_t) \tag{29}$$

$$y_t = A c_t^{\alpha} (\omega_{t-1} + s_t + r_t - c_t)^{\beta} \tag{30}$$

$$\omega_t = \omega_{t-1} + s_t + r_t - c_t \tag{31}$$

Now let

$$s_t \equiv \ell_t \omega_{t-1},\ r_t \equiv q_t \omega_{t-1},\ c_t \equiv e_t \omega_{t-1}, \tag{32}$$

The rates ℓ_t, q_t, and e_t can potentially vary with t.

By equations (31) and (32),

$$\omega_t = \omega_{t-1}(1 + \ell_t + q_t - e_t) \tag{33}$$

Given the notation above, the Bellman equation is

$$\begin{aligned} U_t(\omega_{t-1}) = \max_{e,t,q_t} \ & \{\alpha \log(e_t) + \beta \log(1 + q_t + \ell_t - e_t\ ) + \theta \log(1 - q_t) \\ & + (\alpha + \beta + \theta) \log(\omega_{t-1}) + \delta\ U_{t+1}(\omega_t)\} \end{aligned} \tag{34}$$

7.1.1 Derivation of Optimal Land Carbon Emissions Rate e_t

The first order condition in e_i is

$$\frac{\alpha}{e_t} - \frac{\beta}{1 + \ell_t + q_t - e_t} = \delta \frac{\partial U}{\partial \omega_t} \omega_{t-1} \tag{35}$$

Differentiating the value function,

$$\begin{aligned}\frac{\partial U}{\partial \omega_t} &= \frac{\alpha+\beta+\theta}{\omega_t} + \delta\frac{\partial U}{\partial \omega_{t+1}}(1+\ell_{t+1}+q_{t+1}-e_{t+1}))\\ &= \frac{\alpha+\beta+\theta}{\omega_t} + \left(\frac{\alpha}{e_{t+1}} - \frac{\beta}{1+\ell_{t+1}+q_{t+1}-e_{t+1}}\right)\frac{1}{\omega_t}(1+\ell_{t+1}+q_{t+1}-e_{t+1})\\ &\quad \text{(second equality is from substituting FOC one period forward.)}\end{aligned} \tag{36}$$

Substituting (36) into the FOC (35), we obtain

$$\begin{aligned}&\frac{\alpha}{e_t} - \frac{\beta}{1+\ell_t+q_t-e_t}\\ &= \delta\frac{\omega_{t-1}}{\omega_t}\left[(\alpha+\beta+\theta) + \left(\frac{\alpha}{e_{t+1}} - \frac{\beta}{1+\ell_{t+1}+q_{t+1}-e_{t+1}}\right)(1+\ell_{t+1}+q_{t+1}-e_{t+1})\right]\\ &= \frac{\delta\omega_{t-1}}{\omega_{t-1}(1+\ell_t+q_t-e_t)}\left[(\alpha+\beta+\theta) + \left(\frac{\alpha}{e_{t+1}} - \frac{\beta}{1+\ell_{t+1}+-e_{t+1}}\right)(1+\ell_{t+1}+q_{t+1}-e_{t+1})\right]\end{aligned} \tag{37}$$

or

$$\frac{\alpha(1+\ell_t+q_t-e_t)}{e_t} - \beta = \delta\left[(\alpha+\beta+\theta)\left(\frac{\alpha(1+\ell_{t+1}+q_{t+1}-e_{t+1})}{e_{t+1}} - \beta\right)\right] \tag{38}$$

Iterating forward yields

$$\frac{\alpha(1+\ell_t+q_t-e_t)}{e_t} - \beta = \frac{\delta}{1-\delta}(\alpha+\beta+\theta) \tag{39}$$

Solving for e_t yields

$$e_t = \frac{\alpha(1-\delta)(1+\ell_t+q_t)}{(1-\delta)(\alpha+\beta)+\delta(\alpha+\beta+\theta)\theta)} \tag{40}$$

We are not yet done since q_t is also an endogenous choice by the country.

7.1.2 Derivation of Optimal Land Carbon Removals Rate q_t

The first order condition in q_t is

$$-\frac{\theta}{1-q_t} + \frac{\beta}{1+\ell_t+q_t-e_t} + \delta\frac{\partial U}{\partial \omega_t}\omega_{t-1} = 0 \tag{41}$$

which we can rewrite as

$$\frac{\theta}{1-q_t} - \frac{\beta}{1+\ell_t+q_t-e_t} = \delta\frac{\partial U}{\partial \omega_t}\omega_{t-1} \tag{42}$$

Once more we differentiate the value function,

$$\begin{aligned}\frac{\partial U}{\partial \omega_t} &= \frac{\alpha+\beta+\theta}{\omega_t} + \delta\frac{\partial U}{\partial \omega_{t+1}}(1+\ell_{t+1}+q_{t+1}-e_{t+1}))\\ &= \frac{\alpha+\beta+\theta}{\omega_t} + \left(\frac{\theta}{1-q_{t+1}} - \frac{\beta}{1+\ell_{t+1}+q_{t+1}-e_{t+1}}\right)\frac{1}{\omega_t}(1+\ell_{t+1}+q_{t+1}-e_{t+1})\\ &\quad \text{(second equality is from substituting FOC one period forward.)}\end{aligned} \tag{43}$$

Substituting (43) into the FOC (42), we obtain

$$\begin{aligned}&\frac{\theta}{1-q_t} - \frac{\beta}{1+\ell_t+q_t-e_t}\\ &= \delta\frac{\omega_{t-1}}{\omega_t}\left[(\alpha+\beta+\theta) + \left(\frac{\theta}{1-q_{t+1}} - \frac{\beta}{1+\ell_{t+1}+q_{t+1}-e_{t+1}}\right)(1+\ell_{t+1}+q_{t+1}-e_{t+1})\right]\\ &= \frac{\delta\omega_{t-1}}{\omega_{t-1}(1+\ell_t+q_t-e_t)}\left[(\alpha+\beta+\theta) + \left(\frac{\theta}{1-q_{t+1}} - \frac{\beta}{1+\ell_{t+1}+-e_{t+1}}\right)(1+\ell_{t+1}+q_{t+1}-e_{t+1})\right]\end{aligned} \tag{44}$$

or

$$\frac{\theta(1+\ell_t+q_t-e_t)}{1-q_t} - \beta = \delta\left[(\alpha+\beta+\theta)\left(\frac{\theta(1+\ell_{t+1}+q_{t+1}-e_{t+1})}{1-q_{t+1}} - \beta\right)\right] \tag{45}$$

Iterating forward yields

$$\frac{\theta(1+\ell_t+q_t-e_t)}{1-q_t} - \beta = \frac{\delta}{1-\delta}(\alpha+\beta+\theta) \tag{46}$$

Notice that this looks a lot like Equation (39). Since the right-hand side of (39) and (46) are the same, we equate the left hand sides to obtain

$$q_t = 1 - \frac{\theta}{\alpha}e_t \tag{47}$$

This is an easy equation that relates the optimal choices of q_t and e_t. Substituting (47) into the equation (40) we obtain

$$e_t = \frac{\alpha(1-\delta)(1+\ell_t+(1-\frac{\theta}{\alpha}e_t))}{(1-\delta)(\alpha+\beta)+\delta(\alpha+\beta+\theta)} \tag{48}$$

Solving for e_t (with a few steps of algebra) we obtain the optimal rate of land carbon extraction

$$e_t^* = \frac{\alpha(1-\delta)(2+\ell_t)}{\alpha+\beta+\theta} \tag{49}$$

Finally, substituting (49) into the equation for q_t, i.e., $q_t = 1 - \frac{\theta}{\alpha}e_t$ from (47) we obtain he optimal rate of atmospheric removal:

$$q_t^* = 1 - \frac{\theta(1-\delta)(2+\ell_t)}{\alpha+\beta+\theta} \tag{50}$$

Multiplying e_t^* and q_t^* by ω_{t-1}^{lan} gives the resulting optimal consumption and removal policies, c_t^* and r_t^*, respectively.

Multiplying both sides of (49) and (50) by the state ω_{t-1}, we we obtain

$$\begin{aligned} c_t^* &= \frac{\alpha(1-\delta)(2\omega_{t-1}+s_t)}{\alpha+\beta+\theta} \text{ and} \\ r_t^* &= \omega_{t-1} - \frac{\theta(1-\delta)(2\omega_{t-1}+s_t)}{\alpha+\beta+\theta} \end{aligned} \tag{51}$$

7.2 Estimating Equation

We show how the optimal choices in (51) can generate a simple estimating equation.

Substitute the functions in (51) into the law of motion. This yields

$$\begin{aligned} \omega_t &= \omega_{t-1} + s_t + r_t^* - c_t^* \\ &= \left(1 - \frac{(1-\delta)(\alpha+\theta)}{\alpha+\beta+\theta}\right)(2\omega_{t-1}+s_t) \end{aligned} \tag{52}$$

Notice that one can separate out the term $2\omega_{t-1} + s_t$ from the parameters. Our estimating equation in logs is (ignoring the scale term A, and fossil fuel and labor, c_t^{fos} and L_t, resp.,

$$\log(y_t) = \alpha \log\left(\frac{\alpha(1-\delta)}{\alpha+\beta+\theta}\right) + \beta \log\left(1 - \frac{(1-\delta)(\alpha+\theta)}{\alpha+\beta+\theta}\right) + (\alpha+\beta)\log(2\omega_{t-1}+s_t) \tag{53}$$

So the first two terms on the right-hand side are constants. The second term has the same coefficient, $\alpha + \beta$ as before, and the data is $2\omega_{t-1} + s_t$ each period. Equation (53) coincides with Equation (12) once the definitions of the coefficients and variables are used. One does not need the data on c_t and r_t to estimate Equation (12).

7.3 Description of the Data

- *Countries.* Country data covers 162 countries that are included in at at least one cluster: Albania, Algeria, Angola, Argentina, Armenia, Australia, Austria, Azerbaijan, Bahamas, Bahrain, Bangladesh, Barbados, Belarus, Belgium, Belize, Benin, Bhutan, Bolivia, Bosnia and Herzegovina, Botswana, Brazil, Brunei Darussalam, Bulgaria, Burkina Faso, Burundi, Cabo Verde, Cambodia, Cameroon, Canada, Central African Republic, Chad, Chile, China, Colombia, Comoros, Congo, Dem. Republic Congo, Costa Rica, Cote d'Ivoire, Croatia, Cuba, Cyprus, Czech Republic, Denmark, Djibouti, Dominican Republic, Ecuador, Egypt, El Salvador, Equatorial Guinea, Estonia, Ethiopia, Fiji, Finland, France, Gabon, Gambia, Georgia, Germany, Ghana, Greece, Guatemala, Guinea, Guinea-Bissau, Guyana, Honduras, Hungary, Iceland, India, Indonesia, Iran, Iraq, Ireland, Israel, Italy, Jamaica, Japan, Jordan, Kazakhstan, Kenya, Korea, Rep., Kuwait, Kyrgyzstan, Laos, Latvia, Lebanon, Lesotho, Liberia, Lithuania, Macedonia FYR, Madagascar, Malawi, Malaysia, Mali, Malta, Mauritania, Mauritius, Mexico, Moldova, Mongolia, Morocco, Mozambique, Myanmar, Namibia, Nepal, Netherlands, New Zealand, Nicaragua, Niger, Nigeria, Norway, Oman, Pakistan, Panama, Papua New Guinea, Paraguay, Peru, Philippines, Poland, Portugal, Romania, Russia, Rwanda, Saint Lucia, Saint Vincent and the Grenadines, Samoa, Saudi Arabia, Senegal, Serbia, Sierra Leone, Singapore, Slovakia, Slovenia, Solomon Islands, South Africa, Spain, Sri Lanka, Sudan, Suriname, Swaziland, Sweden, Switzerland, Tajikistan, Thailand, Togo, Tonga, Trinidad and Tobago, Tunisia, Turkey, Turkmenistan, Uganda, Ukraine, United Arab Emirates, United Kingdom United States of America, Uruguay, Uzbekistan, Vanuatu, Venezuela, Viet Nam, Zambia, Zimbabwe.

- *Units of Measurement.* Unless otherwise noted, the units of measurement are gigatonnes (GtC or 10^9 metric tonnes) of carbon dioxide equivalent (C02e). Units of C02e convert all green house gases (CH4 Methane, CO2 Carbon Dioxide, N2O Nitrous Oxide, and three fluorinated gases: Hydrofluorocarbons, Perfluorocarbons, and Sulfur Hexafluoride) into CO2 by measuring Global Warming Potential (GWP), a relative measure of how much heat a greenhouse gas traps in the atmosphere. It compares the "amount of heat trapped by a certain mass of the gas in question to the amount of heat trapped by a similar mass of carbon dioxide." Using Global Warming Potential, one unit of carbon translates roughly to 3.67 units of CO2.

  In all the series below, a length of time is five years (though for some purposes,

annual rolling five year aggregates are used). Thus, flow data is a five year aggregated flow. Carbon stock data is the value given in the particular year. When time periods are quinquennial (5 year intervals), stock data are given for years at the end of a quinquennial time period, for instance, stock data for the period 1991-1995 is the stock year 1995. Flow data ending in 1995 aggregates the annual flows in a quinquennial time period, e.g., the yearly flows from 1991 to 1995. The reason for using 5 year intervals is that FAOSTAT data conforms to U.N. reporting requirements of five year increments, each date t represents the end of a five year period up to and including the current year. In particular, the UNCCC reporting procedures require countries to update their carbon measurement every 5 years, typically in years ending in 0 or 5. measurements typically occur in years 1990, 2000, 2005, 2010, and 2015. While FAOSTAT does report annual data, the data in the intervening years appears to be extrapolated from the quinquennial reports.

In what follows, "t" indexes quinquennial dates $1990, 1995, \ldots, 2015$ and "τ" indexes annual dates, $1990, 1991, 1992, \ldots, \ldots, 2015$.

- *Annual data on five-year aggregated global land sink* $\tilde{s}_\tau^{lan}$: The data on global annual sink s_τ^{lan} comes from the Le Quere et al. (2018) linked from the Global Carbon Project 2018 (GCP 2018). GCP 2018 data is annual. The sink s_τ^{lan} (with τ representing a period of a year) is "estimated by the difference of the other terms of the global carbon budget and compared to results of independent Dynamic Global Vegetation Models forced by observed climate, CO2 and land cover change (some including nitrogen-carbon interactions)..."[20] The data used in for our estimation are five year flows up to and including τ so that $\tilde{s}_\tau^{lan} = \sum_{j=0}^{4} s_{\tau-j}$. Annual data on 5-year rolling aggregates is needed to obtain large enough sample sizes for estimation (see Appendix 7.5.1 for details).

- *Annual global land carbon stock* ω_τ^{lan}: The global land stock data is annual from 1982 to 2015. For consistency, changes in ω_τ^{lan} are from the same source (GCP 2018) as s_τ^{lan}. The series for ω_τ^{lan} is then constructed from a benchmark value set at FAO Forest Carbon stock in the base year 2000. Additions and subtractions from the base year are then determined annually by land emissions (land use − land sink) series from GCP 2018 (the same source as for s_t^{lan}), dating back to 1982. Net land emissions are subtracted forward and added backward from the base year to obtain an annual series from 1982 to 2015.[21] The annual data

[20] Le Quere et al. (2016), p. 3.

[21] Note that a similar series from the FAO is inadequate. It interpolates between five year periods

is used for constructing the 5 year rolling aggregate $\tilde{s}^{lan}_{tau}, \omega^{lan}_{\tau-5}$ land sink rate as τ varies annually from 1990-2015.

- *Quinquennial country land carbon stocks* ω^{lan}_{it}: The data at quinquennial intervals from 1990 to 2015 comes from FAOSTAT, the database for the Food and Agricultural Organization (FAO). FAOSTAT contains data on Forest Carbon stock in living (above and below ground) biomass for each country and derived from the FAO Forest Resource Assessments (FAO FRA). The data measures only living biomass in forests. See http://www.fao.org/faostat/en/#data. Data on soils, leaf litter is found in FAO's Global Forest Resource Assessment 2015 for the single year 2015. Data on biomass on agricultural land is found in Zomer et al. (2016) for the years 2000 and 2010. Forest biomass is significantly larger than agricultural biomass in most countries. In 2010 in the U.S. the agricultural carbon stock is 9.5% of the total. In Brazil, 11.5%. In India, however, agricultural biomass is 41%.

- *Quinquennial, 5-year aggregated country land sink* $\tilde{s}^{lan}_{it}$: The model posits absorption efficiency per unit land carbon biomass to be identical across all country's stocks, global land sink data is used to compute country-specific sinks per unit carbon biomass. Specifically, for quinquennial dates t, $\frac{\tilde{s}^{lan}_{it}}{\omega^{lan}_{it-5}} = \frac{\tilde{s}^{lan}_{t}}{\omega^{lan}_{it-5}}$. With the data on land stocks and on the global sinks, the country specific land sink is constructed.

- *Quinquennial atmospheric GHG stock* ω^{amt}_{t}: Annual data on global GHG atmospheric (CO2e) stocks from 1982 to 2016 are taken from NOAA Earth Systems Research Laboratory,

  https://www.esrl.noaa.gov/gmd/ccgg/trends/global.html.

  The NOAA report is a time series of atmospheric CO2e levels from the Moana Loa Observatory. Data is expressed in parts per million by volume (ppm). To convert from ppm to gigatonne of carbon, the conversion tables of the Carbon Dioxide Information Analysis Center advise that 1 part per million of atmospheric CO2e is equivalent to 7.81 Gt CO2e. The GHG concentrations include non-carbon GHGs contributing to temperature rises that determine land sink absorption rate. The index t is over quinquennial dates.

from 1990 to 2015 and so has six distinct data points. The constructed series by contrast is annual data from 1982-2015.

- *Quinquennial, 5-year aggregated fossil fuel emissions* $\{\tilde{c}_{it}^{fos}\}$: Data on fossil fuel consumption for each country is from the CAIT Climate Data Explorer, 2017, the database provided by the World Resources Institute, http://cait.wri.org/historical. From this data we construct five year flows for our estimation. Recall that $\tilde{c}_{it}^{fos}$ is the five year sum: $\tilde{c}_{it}^{fos} = \sum_{j=0}^{4} c_{i,\tau-j}^{fos}$.

- *Quinquennial 5-year aggregated output* $\tilde{y}_{it}$ *and quinquennial labor* L_{it}: Annual GDP and labor country data taken from the World Bank database. GDP is in 2015 constant dollars. From this data we construct five year flows for output: $\tilde{y}_{it} = \sum_{j=0}^{4} y_{i,\tau-j}$. Labor is a stock variable and so variable and so L_{it} is the labor force at quinquennial date t.

Notes. Agricultural carbon stock is excluded. Data fromZomer et al. (2016) only covers two years, 2000 and 2010. In the U.S. agricultural stock was measured by Zomer to be 6.34 GtCO2e in 2000 and 6.62 Gt CO2e in 2010. Forestry stock in those two years measured measured 57.66 and 62.64 in those years, resp. Hence agricultural stock comprised 10% and 9.5% of the total carbon stocks in those years.

7.4 Estimation Details and Results

The derivation of the estimating equation in Appendix 7.2 produces the estimating equation (27). In the equation, B_{i0} is the country-fixed dummy for country i. The remaining coefficients can be expressed as $B_{k_s1}, B_{k_s2}, B_{k_s3}$ correspond to the cluster k_s in the clustering strategy s. OLS estimates (with country-fixed effects) of these parameters are obtained in MATLAB for 8 clustering strategies in all. The clustering strategies are, in order,

1. Global sample. There is a single k with all 162 countries. (Table 2).

2. Human Development Index (HDI). k ranges over four clusters are High, Medium High, Medium Low, and Low development groups (Table 2).

3. HDI binary. This strategy groups High and Medium High HDI clusters together, and Low and Medium Low clusters together.

4. OECD Membership. Binary partition. Either includes or excludes country.

5. Top 30 GDP countries. Binary partition. Either includes or excludes country.

6. Top 30 GHG emitters. Binary partition. Either includes or excludes country.

Table 5: Estimated Policy-Adjusted Production Coefficients by Binary Human Development Index Cluster.

	Dependent Variable - Log GDP	
Coefficients	High HDI	Low HDI
B_1 Carbon Stock	0.889***	0.041
	(0.103)	(0.107)
B_2 Fossil Fuel	0.870***	1.037***
	(0.090)	(0.085)
B_3 Labor Force	0.327***	0.695***
	(0.097)	(0.103)
Observations	455	355
R^2	0.995	0.995
F Statistic	596.8	563.6

Standard errors in parentheses. Symbols *, **, and *** indicate statistically significant at the 10%, 5%, and 1% levels, respectively.

7. Top 35 Forested countries. Binary partition based on total Gt C in each country. Either includes or excludes country.

8. Geographic cluster. Six groupings: North America (excluding Mexico). Central and South America (including Mexico), Europe, Asia, Oceana, Africa.

All data, including membership list for each cluster in each of the 8 strategies is available upon request.

Table 2, in the text, reports on results for the global and HDI cluster (strategies 1 and 2 listed above). The results for subsequent 6 clusters are in following tables, Tables 5-10:

7.5 Details of the Simulations and Figures

7.5.1 Land Sink Estimation

Restricting attention to the quinquennial periods from 1990 to 2015, a reasonable sample size is obtained by estimating the quinquennial flows *annually* since 1982.

Table 6: Estimated Policy-Adjusted Production Coefficients by OECD Membership.

	Dependent Variable - Log GDP	
Coefficients	OECD	Non-OECD
B_1 Carbon Stock	0.723***	0.153***
	(0.099)	(0.088)
B_2 Fossil Fuel	0.093	1.143***
	(0.108)	(0.072)
B_3 Labor Force	1.251***	0.440***
	(0.156)	(0.078)
Observations	165	635
R^2	0.997	0.994
F Statistic	934.3	518.8

Standard errors in parentheses. Symbols *, **, and *** indicate statistically significant at the 10%, 5%, and 1% levels, respectively.

Table 7: Estimated Policy-Adjusted Production Coefficients by Gross Domestic Product.

	Dependent Variable - Log GDP	
Coefficients	Top 30 GDP Countries	Other Countries
B_1 Carbon Stock	1.061*	0.324***
	(0.134)	(0.082)
B_2 Fossil Fuel	0.827***	0.986***
	(0.089)	(0.077)
B_3 Labor Force	0.161**	0.701***
	(0.107)	(0.083)
Observations	150	660
R^2	0.991	0.993
F Statistic	301.5	402.1

World Bank 2016 Rankings. Standard errors in parentheses. Symbols *, **, and *** indicate statistically significant at the 10%, 5%, and 1% levels, respectively.

Table 8: Estimated Policy-Adjusted Production Coefficients by GHG Emissions.

	Dependent Variable - Log GDP	
Coefficients	Top 30 GHG-Emitting Countries	Other Countries
B_1 Carbon Stock	0.747***	0.352***
	(0.132)	(0.083)
B_2 Fossil Fuel	1.084***	0.927***
	(0.092)	(0.077)
B_3 Labor Force	-0.010	0.764***
	(0.113)	(0.083)
Observations	145	665
R^2	0.990	0.993
F Statistic	281.8	398.8

EDGAR database, 2017. Standard errors in parentheses. Symbols *, **, and *** indicate statistically significant at the 10%, 5%, and 1% levels, respectively.

Table 9: Estimated Policy-Adjusted Production Coefficients by Inclusion among Top 35 Forested Countries.

	Dependent Variable - Log GDP	
Coefficients	Top 35 Forested Countries	Other Countries
B_1 Carbon Stock	0.263	0.405***
	(0.304)	(0.078)
B_2 Fossil Fuel	0.950***	0.975***
	(0.109)	(0.079)
B_3 Labor Force	0.883***	0.575***
	(0.142)	(0.084)
Observations	175	635
R^2	0.997	0.994
F Statistic	859.5	505.1

Rankings in Global Forest Resources Assessment 2015, FAO. Standard errors in parentheses. Symbols *, **, and *** indicate statistically significant at the 10%, 5%, and 1% levels, respectively.

Table 10: Estimated Policy-Adjusted Production Coefficients by Geographic Region.

	Dependent Variable - Log GDP					
Coefficients	NA	SA	AS	EU	AF	OC
B_1 Carbon Stock	1.665***	0.560***	0.071	1.441***	-0.042	0.158
	(0.220)	(0.131)	(0.167)	(0.146)	(0.122)	(0.208)
B_2 Fossil Fuel	0.970***	0.774***	1.417***	0.530***	0.970***	0.585*
	(0.296)	(0.106)	(0.133)	(0.144)	(0.100)	(0.381)
B_3 Labor Force	1.471***	0.862***	0.145	-0.040	0.717***	0.777***
	(0.156)	(0.117)	(0.136)	(0.244)	(0.120)	(0.306)
Observations	10	140	195	195	235	35
R^2	0.999	0.999	0.992	0.994	0.994	0.999
F Statistic	31995.6	1957.4	349.3	433.0	448.5	1478.6

Standard errors in parentheses. Symbols *, **, and *** indicate statistically significant at the 10%, 5%, and 1% levels, respectively. NA: North America. SA: South and Central America. AS: Asia. EU: Europe. AF: Africa. OC: Oceania.

Recall that the annual 5-year rolling aggregate for global land sink is defined as

$$\tilde{s}_{\tau}^{lan} = \sum_{j=0}^{4} s_{\tau-j}^{lan} \tag{54}$$

for τ annual. In addition,

$$\widetilde{\rho}_{\tau}^{lan} = \frac{\tilde{s}_{\tau}^{lan}}{\omega_{\tau-5}^{lan}} \tag{55}$$

which is assumed identical across countries.

In other words, $\widetilde{\rho}_{\tau}^{lan}$ is the quinquennial absorption rate based on the land sink summed over the five year period up to and including annual date τ. τ. We estimate the analogue of Equation (28), namely

$$\widetilde{\rho}_{\tau} = \pi_0 + \pi_1 \omega_{\tau-5}^{atm} + \pi_2 (\omega_{\tau-5}^{atm})^2 + \nu_{\tau} \tag{56}$$

where τ is the standard period length of a year, and we assume $E[\nu_{\tau}|\omega_{\tau-5}^{atm}] = 0$. The equation system is a rolling aggregate of 5 year flows and end-of-period stocks for each period τ where τ varies yearly from 1987-2016, and the data series for all stocks start in 1982.

Estimation of (56) is by OLS. The rolling aggregate structure induces serial correlation in errors so that OLS will generally be inefficient. With additional assumptions on the covariance matrix, (56) can be re-estimated by GLS.

7.5.2 Data Projections Used in the Simulation

The paths for $\{\tilde{y}_{it}\}$ and $\{\omega_{it}^{lan}\}$ are simulated for $t = 2020, 2025, 2030, \ldots, 2100$ under four RCP scenarios, each corresponding to Global Radiative Forcing levels 2.5, 4.5, 6.0, and 8.5, respectively, in the year 2100. The ingredients required for the simulation are:

7.5.3 *Parameter Estimates from the Model*

$\hat{B}_0$, $\hat{B}_1$, $\hat{B}_2$, $\hat{B}_3$ for countries in a given cluster, and $\hat{\pi}_0$, $\hat{\pi}_1$, and $\hat{\pi}_2$ from the land sink equation.

7.5.4 *Exogenous Forecasts for Series* $\{L_{it}\}$

.

Forecasted series $\{L_{it}\}$. Raw data comes from the U.N. Databank and the World Bank and constructed as follows. The projected labor force for 194 countries, from 2020 to 2100, is based on the following methodology: the UN databank projects male and female labor until 2100. Then take the 2017 labor force participation rates of men and women by age ranges 15-64 and 65+ to account for differences between participation rates between adults and senior population. Participation data is from the World Bank. Countries are the clustered by HDI. Participation rates of the 194 countries (by age group and sex) are assumed to converge to the average participation rate of high income developed countries, based on the assumption that they had already achieved a steady state of this rate. The convergence year depend on the classification of the countries. Specifically, High HDI converge in 2020, High Middle HDI converge in 2040, Low middle HDI converge in 2070 and Low HDI in 2100. Finally, labor force is the product of the participation rate and the projected projected population for each period.

7.5.5 *RCP Forecast Scenarios for* $\{\omega_t^{atm}\}$

The RCPs are four independent pathways developed by four individual modeling groups.

- RCP 2.6: Stipulates peak radiative forcing at $\approx\ 3W/m^2$ before declining to $2.6W/m^2$ by 2100. RCP 2.6 represents mitigation scenarios with full from all countries to limit the increase of global mean temperature to $2°C$. It forecasts negative energy use emissions growth in the second half of the 21st century due to a low carbon factor (carbon per energy unit), low energy intensity (energy

use per dollar income) and low population growth. The economic part assumes that market share of a certain technology or fuel type depends on costs relative to competing technologies. Reference: van Vuuren et al. (2006, 2007).

- RCP 4.5: Stabilizes radiative forcing at $4.5W/m^2$ in 2100 without ever exceeding that value (no overshooting). The economic model is a cost-minimizing policy pathway that reaches the target radiative forcing. The cost-minimizing policy drives changes in the energy system, including shifts to electricity, to lower emissions energy technologies and to the deployment of carbon capture and geologic storage technology. Emissions pricing also applies to land use emissions; as a result, forest lands expand from their present day extent. Reference: Clarke et al. (2007), citetSmithWigley06, and Wise et al. (2009).

- RCP 6.0. Stabilizes radiative forcing at $6.0W/m^2$ by 2100, without overshooting. It uses AIM/CGE which models a disaggregated energy system with both supply and demand sides. The pathway is achieved in a general equilibrium model with non-forward-looking agents, and with technology-explicit modules in power sectors. Source: Fujino et al. (2006) and Hijioka et al. (2008).

- RCP 8.5. Stipulates a rising radiative forcing pathway leading to $8.5W/m^2$ in 2100. RCP 8.5 uses the IAM, MESSAGE and forecasts higher carbon factor, energy intensity, and population growth. The economic model consists of forward looking, representative-agent optimization to obtain consumption, savings, and investment. Source: Riahi and Nakicenovic (2007).

Notes. The database for the RCPs is housed at International Institute for Applied Systems Analysis (IIASA). According to their site[22]

> "The RCPs, which replace and extend the scenarios used in earlier IPCC assessments [prior to AR5], are compatible with the full range of stabilization, mitigation, and baseline emission scenarios available in the current scientific literature."

The database itself is found at https://tntcat.iiasa.ac.at/RcpDb (accessed 2-20-2019). The RCPs aggregate at the regional/development level, dividing countries according to five categories: the OECD 90 (includes the expanded list of OECD countries, the reforming economies (mostly Eastern Europe), Asia, Middle East and Africa, and Latin America.

[22] http://www.iiasa.ac.at/web/home/research/researchPrograms/TransitionstoNewTechnologies/RCP.en.html, accessed 2-20-2019.

Various disclaimers on that site note RCPs are "not new, fully integrated scenarios (i.e., they are not a complete package of socioeconomic, emissions, and climate projections)." and "do not represent specific futures with respect to climate policy action (or no action) or technological, economic, or political viability of specific future pathways or climates." (Characteristics and guidance, https://tntcat.iiasa.ac.at/RcpDb.

7.5.6 *RCP Data for Series* $\{\tilde{c}_{it}^{fos}\}$

.

There are four distinct series each based in one of the four RCPs (see sources for each RCP).

The construction of $\tilde{c}_{it}^{fos}$ is done by estimating the decadal percentage variation of GHG emissions, excluding LUCF, for each region in each RCP. These growth rates are then attributed to each country within that region. To account for the different GHGs we convert each gas into CO2e units using standard conversion factors from global warming potential as specified in the IPCC 5th Assessment Report.

The equation below for the change Δ in fossil fuel emissions describes which gases are included. For region j we define

$$\Delta_{j,t,RCP} = \text{CO2 fossil fuel}_{j,t,RCP} + \left(\text{total CH4} - \underbrace{(\text{CH4 from grassland and forest burn})}_{\text{LUCF}} \right)_{j,t,RCP} + \text{other GHGs}_{j,t,RCP}\Big|_{\text{all as CO2e}} \tag{57}$$

Then the $\tilde{c}_{ijt,RCP}^{fos}$ of the country i that belong to the region j under the RCP, when $t \in \{2020, 2030, 2040, \ldots, 2100\}$ is given by:

$$\tilde{c}_{i,j,t+10,RCP}^{fos} = \tilde{c}_{ijt,RCP}^{fos} \frac{\Delta_{j,t+10,RCP} - \Delta_{j,t,RCP}}{\Delta_{j,t,RCP}}$$

Then for mid-decade dates $t \in \{2025, 2035, 2045, \ldots, 2095\}$ the projection for fossil fuel is given by:

$$\tilde{c}_{it,RCP}^{fos} = \alpha \tilde{c}_{i\,t-5,\,RCP}^{fos} + (1-\alpha)\tilde{c}_{it+5,RCP}^{fos},$$

with $\alpha = 0.5 \in (0, 1)$.

7.5.7 Simulation Algorithm

The basic steps of the simulation are described here. The Appendix fills in the details.

Step 1. The constructed series for each RCP corresponds to sequences $\{\tilde{c}^{fos}_{it,RCP}\}$ and $\{\omega^{atm}_{t,RCP}\}$ where $t = 2020, 2025, 2030, \ldots, 2100$.

Step 2. Let

$$\widehat{\widetilde{\rho}}_{t,RCP} = \hat{\pi}_0 + \hat{\pi}_1 \omega^{atm}_{t-5,RCP} + \hat{\pi}_2 (\omega^{atm}_{t-5,RCP})^2 \tag{58}$$

denoting the predicted value of the land sink absorption rate under the RCP forecast $\{\omega^{atm}_{t,RCP}\}$ and estimates $\hat{\pi}_0$, $\hat{\pi}_1$, and $\hat{\pi}_2$ $\hat{\pi}_2$ of the land sink sequestration equation.

Step 3. Estimate a parameter, in-sample, from the law of motion of land under optimal land policy. Combining the stock law of motion in (5) with optimal land use policies in (10) in the Proposition, one obtains one obtains

$$\begin{aligned} \omega^{lan}_{it} &= \omega^{lan}_{it-5} - \tilde{c}^{*lan}_{it}(\omega^{lan}_{it-5}) + \tilde{r}^{*lan}_{it}(\omega^{lan}_{it-5}) + \tilde{s}^{lan}_{it}\tilde{s}^{lan}_{it} \\ &= D_i \left(2\omega^{lan}_{i\,t-5} + \tilde{s}^{lan}_{it}\right) \\ &= D_i \omega^{lan}_{i\,t-5} \left(2 + \widetilde{\rho}_t\right) \end{aligned} \tag{59}$$

where $D_i \equiv 1 - \frac{(1-\delta)(\alpha_i+\theta_i)}{\alpha_i+\beta_i+\theta_i}$ is the model-generated adjustment factor. This is independent of t. Equation (59) describes the theoretical carbon stock dynamics under optimal land use. The evolution of ω^{lan}_{it} depends on the land carbon adjustment factor D_i derived from land use. The *empirical adjustment factor* D_{it} from sample data is

$$D_{it} \equiv \frac{\omega^{lan}_{it}}{\omega^{lan}_{i\,t-5}\left(2 + \widehat{\widetilde{\rho}}_t\right)}. \tag{60}$$

which, unlike the model generated parameter, will generally depend on t due to shocks.

To be consistent with our earlier assumption that parameters $\alpha_i, \beta_i, \gamma_i, \theta_i, \phi_i$ are identical within clusters, we average these empirical adjustment factor over four time periods, 2000, 2005, 2010, 2015, and over all countries in a given cluster k, using HDI as our partition. Thus *average adjustment factor* D_k cluster k is computed as:

$$D_k \equiv \frac{1}{4 \times \#\{\text{ i in cluster k }\}} \sum_{t \in 2000}^{2015} \sum_{i \in \text{cluster}_k} D_{it} \tag{61}$$

The computations of these average adjustment factors across HDI clusters are displayed in Table 11.

Table 11: Mean Adjustment Factors under Optimal Land Policies.

	High HDI	Med High HDI	Med Low HDI	Low HDI
Adjustment Factor D_k	0.5196	0.5062	0.4816	0.4727
	(0.0477)	(0.0604)	(0.0368)	(0.0598)

Standard deviations (not standard errors) in parentheses.

Step 4. Generate the RCP forecasted series $\{\tilde{\omega}^{lan}_{it,RCP}\}$ recursively using the equation

$$\omega^{lan}_{it,RCP} = D_k \omega^{lan}_{it-5,RCP}[2 + \widehat{\widetilde{\rho}}_{t,RCP}] \tag{62}$$

starting from $t - 5 = 2015$, with each t representing a quinquennial time period.

Step 5. Combine series the $\{\omega^{lan}_{it,RCP}\}$, $\{\widehat{\widetilde{\rho}}_{t,RCP}\}$, with the two series $\{L_{it}\}$ $\{\tilde{c}^{fos}_{it,RCP}\}$ with estimates $\hat{B}_0$, $\hat{B}_1$, $\hat{B}_2$, $\hat{B}_3$ from the reduced form equation (12) to generate $\{\tilde{y}_{t,RCP}\}$.

7.5.8 Simulation Figures

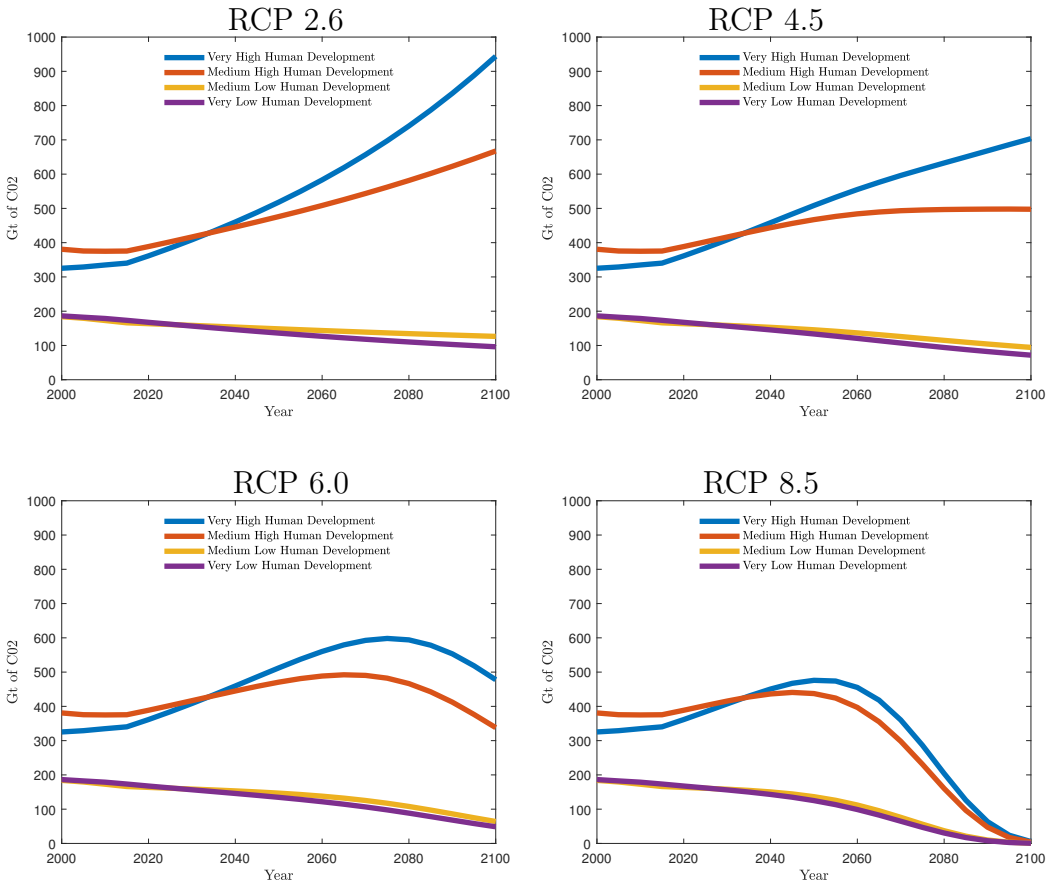

Figure 11: Land Carbon Stock by IPCC-RCP Scenario under HDI Clustering.

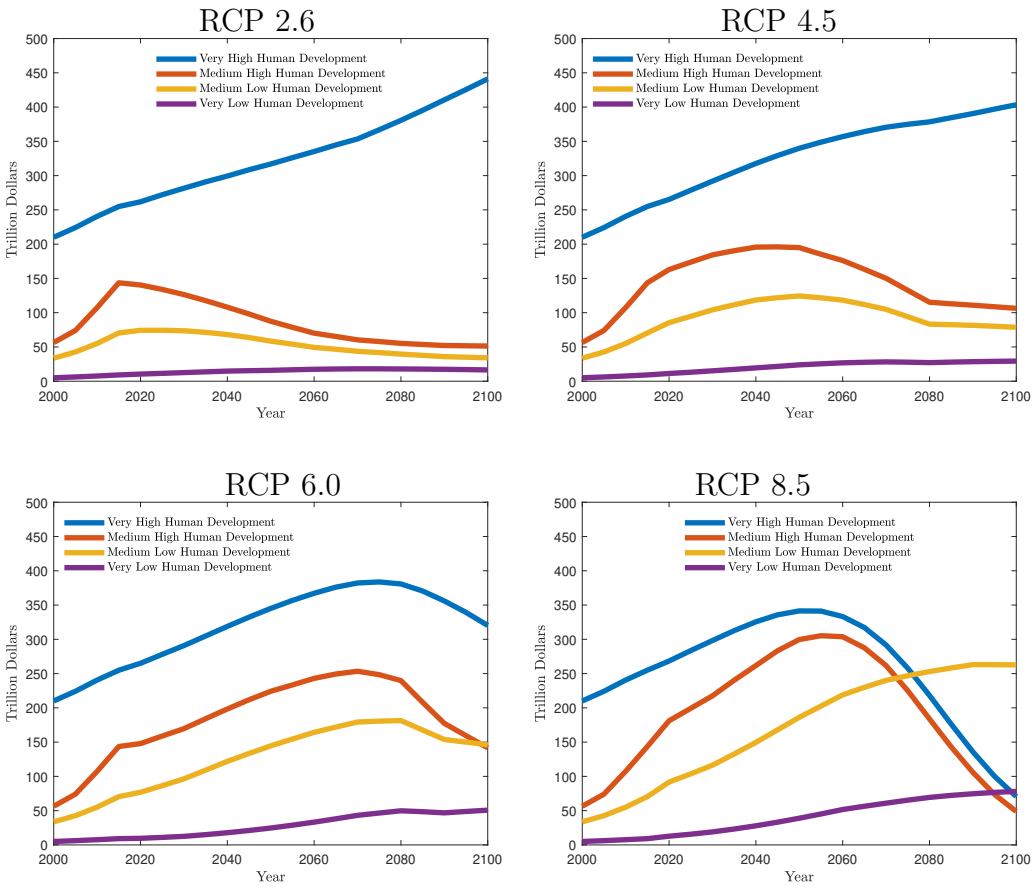

Figure 12: Quinquennially Aggregated GDP by IPCC-RCP Scenario under HDI Clustering.

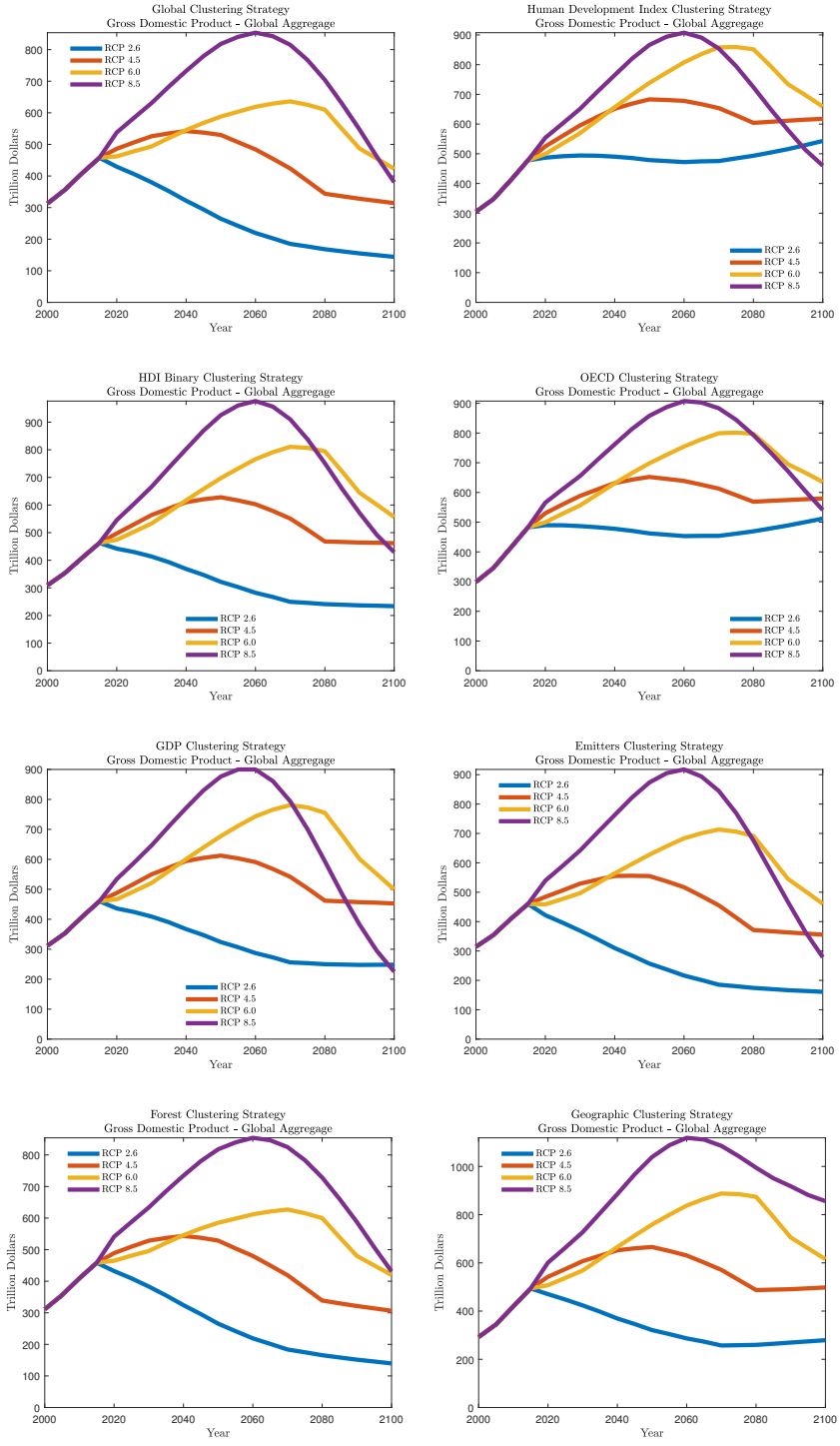

Figure 13: Global GDP by Cluster Strategy, Aggregated Quinquennially and Across Clusters.